J. Condensed Matter Nucl. Sci. 1 (2007) 27–40

Research Article

Nuclear Reactions in Condensed Matter: A Theoretical Study of D–D Reaction within Palladium Lattice by Means of the Coherence Theory of Matter

Fulvio Frisone*

Department of Physics, University of Catania, Via Santa Sofia 64, I-95025 Catania, Italy

Abstract

In the last decades, an indisputable experimental evidence was built up for Low-Energy Nuclear Reaction (LERN) phenomena in specialized heavy hydrogen systems. Actually, the real problem is that, the theoretical statements of LERN are not known; in fact, no new branch of science has begun, yet. In this work, we seek to analyse the deuteron–deuteron reactions within palladium lattice by means of Preparata model of palladium lattice and we will show the occurrence probability of fusion phenomena according to more accurate, but not claimed, experiments, in order to demonstrate theoretically the possibility of cold fusion. Further, we focus on tunnelling the Coulomb barrier existent between two deuterons. Analysing the possible contributions of lattice on improving the tunnelling probability, we will find that there is a real mechanism through which this probability could be increased: this mechanism is the screening effect due to d-shell electrons of palladium lattice. Finally the good agreement between theoretical and experimental results proves the reality of cold fusion phenomena and the reliability of our model.

Keywords: Collective plasmonic excitation, Dislocations, Fusion within a microcrack, Nuclear reaction, Tunneling effect, Vibrational frequency of the lattice

1. Introduction

We have studied that within the Coherence Theory of Condensed Matter it was verified the cold fusion [1–4] phenomena. In this theory [5] it is assumed that the electromagnetic (e.m.) field, due to elementary constituents of matter (i.e. ions and electrons), plays a very important role on dynamic system. In fact considering the coupling between e.m. equations, because of charged matter, and the Schrödinger equation of field matter operator, it is possible to demonstrate that in proximity of e.m. frequency ω_0, the matter system shows a dynamic coherence. That is why it is possible to speak about the coherence domains whose length is about $\lambda_{CD} = 2\pi/\omega_0$.

Obviously, the simplest model of matter with coherence domain is the plasma system. In the usual plasma theory, we have to consider the plasma frequency ω_p and the Debey length that measures the Coulomb force extension, i.e. the

*E-mail: Frisone@ct.infn.it

coherence domain length. In order to address the crucial issue of the nuclear fusion reaction involving the deuterons that pack the Pd-lattice we must have a rather detailed understanding of the environment in which such nuclear process will eventually take place.

For a system with N, charge Q and mass m within a volume (V) the plasma frequency can be written as

$$\omega_{\bar{\mathrm{k}}} = \omega_{\mathrm{p}} = \frac{Qe}{\sqrt{m}}\sqrt{\frac{N}{V}}. \tag{1}$$

Introducing the dimensional variable $\tau = \omega_{\mathrm{p}} t$ we can rewrite the above equations

$$\dot{\phi}_{\vec{n}}(\tau) = \frac{1}{2} \sum_{|\vec{k}|=\omega_{\mathrm{p}}} \sum_{\vec{n}'r} \langle \vec{n} | \alpha_{kr} \vec{\varepsilon}_{kr} \vec{a}^{+} - \alpha^{*}_{kr} \vec{\varepsilon}_{kr} \vec{a} | \vec{n'} \rangle \phi_{\vec{n}'}(\tau), \tag{2}$$

$$\frac{1}{2}\ddot{\alpha}_{kr} - i\dot{\alpha}_{kr} + m\lambda\alpha_{kr} = \frac{i}{2}\vec{\varepsilon}^{*}_{kr} \sum_{\vec{n}\vec{n'}} \langle \vec{n} | \vec{a} | \vec{n'} \rangle \phi^{*}_{\vec{n}}(t) \phi_{\vec{n}'}(\tau), \tag{3}$$

which, defining the state:

$$|\phi\rangle = \sum_{\vec{n}'} \phi_{\vec{n}}(\tau)\, |\vec{n}\rangle \tag{4}$$

and the e.m. field amplitude:

$$\vec{A} = \sqrt{\frac{3}{8\pi}} \sum_{r} \int \mathrm{d}\Omega_k\, \alpha_{kr} \vec{\varepsilon}_{kr}, \tag{5}$$

we can rewrite

$$\frac{\partial}{\partial t}\, |\phi\rangle = \sqrt{\frac{2\pi}{3}} \left(\vec{A}\vec{a}^{+} - \vec{A}^{+}\vec{a} \right) |\phi\rangle\,, \tag{6}$$

$$\dot{\vec{A}} + \frac{i}{2}\ddot{\vec{A}} + im\lambda\vec{A} = -\sqrt{\frac{2\pi}{3}}\, \langle\phi|\, \vec{a}\, |\phi\rangle\,. \tag{7}$$

If we only concentrate on one short time dynamics we can write:

$$|\phi(0)\rangle = |0\rangle\,, \tag{8}$$

then, creating a difference in Eq. (6) and using Eq. (7) with $|\phi\rangle = |0\rangle$, we can easily obtain:

$$\ddot{A}_j + \frac{i}{2}\dddot{A}_j = -\left(\frac{2\pi}{3}\right) \langle 0| \left[a_j, a_l^{+}\right] |0\rangle\,, \tag{9}$$

$$A_l = -\left(\frac{2\pi}{3}\right) A_j. \tag{10}$$

They have the same form of the equations of the coherence domains in the case in which:

$$\mu = 0,$$

$$\lambda = 0,$$

$$g^2 = \left(\frac{2\pi}{3}\right),$$

$$g_c{}^2 = \frac{16}{27} < \frac{2\pi}{3}.$$

Then, a solution for the ideal plasma exists. At any rate defining:

$$\alpha_k = \langle\phi|\, a_k\, |\phi\rangle\,, \tag{11}$$

$$g_0 = \left(\frac{2\pi}{3}\right)^{1/2}.$$

In this case the coupling critical constant of the system is

$$\dot{\alpha}_k = g_0 A_k, \tag{12}$$

$$\dot{A}_k + \frac{i}{2}\ddot{A}_k = -g_0\alpha_k, \tag{13}$$

so to admit the following holding quantity:

$$Q = \sum\left\{A_k^* A_k + \frac{i}{2}\left(A_k^*\dot{A}_k - \dot{A}_k^* A_k\right) + \alpha_k^*\alpha_k\right\}, \tag{14}$$

while for the Hamiltonian's it is easy to compute:

$$\frac{E}{N\omega_p} = H = Q + \sum\left[\frac{1}{2}\dot{A}_k^*\dot{A}_k - ig\left(A_k^*\alpha_k - A_k\alpha_k^*\right)\right]. \tag{15}$$

With the objective of seeing if there are any externals solutions, we write

$$\alpha_k = \alpha u_k e^{i\psi}, \tag{16}$$

$$A_k = A u_k e^{i\phi}, \tag{17}$$

where α and A are positive constants and u_k is a complex vector.

Changing these ones in Eqs. (12) and (13) we have:

$$\phi - \psi = \frac{\pi}{2}, \tag{18}$$

$$\alpha = g_0\frac{A}{\dot{\phi}}, \tag{19}$$

$$\frac{1}{2}\dot{\phi}^3 - \dot{\phi}^2 + g_0^2 = 0, \tag{20}$$

and by the condition $Q = 0$ (we cannot have a net charge flow in a plasma), we have:

$$1 - \dot{\phi} + \frac{g_0^2}{\dot{\phi}^2} = 0. \tag{21}$$

In this case it is easy to observe that for $g_0 = (2\pi/3)^{1/2}$ is unlikely to satisfy both Eqs. (18) and (19).

This result means that the energy of an ideal quantum plasma does not have a minimum; in other words the ideal quantum plasma does not exist.

That is not surprising because the Hamiltonian's describes, of this plasma, a system whose amplitude oscillations are arbitrary, while the limit over a certain amplitude does not exist in a real plasma.

But by:

$$\vec{\xi} = \frac{1}{\sqrt{2m\omega_\mathrm{p}}}(\vec{a} + \vec{a}^+),$$

it is easy to obtain:

$$\left\langle \vec{\xi}^2 \right\rangle = \frac{1}{m\omega_\mathrm{p}}\alpha^2. \tag{22}$$

But in the plasma approximation as an homogeneous fluid, we suppose that our Hamiltonian's stops have to be valid for the oscillations bigger than the following:

$$\left\langle \vec{\xi}^2 \right\rangle_{\max}^{1/2} \approx a = \left(\frac{V}{N}\right)^{1/2} \tag{23}$$

that is when the plasma's oscillations are of the same order of the inter-particle distance a. In order to create some more realistic models of plasma, we want to compute the breaking amplitude $\alpha_{\max}$ obtained by the combination of Eqs. (22) and (23) for a gas of electrons.

Using the definition of ω_p, we have:

$$\alpha_{\max} = \sqrt{m\omega_\mathrm{p}}\left(\frac{1}{3}\right)^{1/3} = (ma)^{1/4}\, e^{1/2} \tag{24}$$

taking

$$a \approx 2.5\ \text{Å}$$

it is calculated

$$\alpha_{\max} \cong 2.7\ \text{Å}.$$

This simple calculation shows how it is possible to change our quantum ideal plasma in a real plasma. For a plasma of electrons the oscillations remain very little and so a two levels model can be a good approximation (the dynamics only includes the first excited state). A consequence of this approximation, consisting in the reduction of the plasma in a homogeneous fluid, is the changing of the plasma frequency ω_{rmp}

$$\omega_\mathrm{p} = \frac{Q}{\sqrt{m}}\sqrt{\frac{N}{V}}. \tag{25}$$

Moreover, we study the "nuclear environment", that it is supposed existent within the palladium lattice D_2-loaded and at room temperature as predicted by Coherence Theory. In fact when the palladium lattice is loaded with deuterium gas, some physicists declared that it is possible to observe traces of nuclear reactions [1–3]. For this reason many of these physicists speak about Low- Energy Nuclear Reaction (LERN).

One of the biggest experiments tell us that in the D_2-loaded palladium case the most frequent nuclear reactions are [3,4]:

(a) $\mathrm{D} + \mathrm{D} \to {}^3\mathrm{H} + \mathrm{p} + 4.03\,\mathrm{MeV}$,

$$\text{(b)} \qquad \mathrm{D} + \mathrm{D} \rightarrow {}^{4}\mathrm{He} + \gamma \text{ (23.85 MeV)}.$$

In our work, we aim to propose a "coherence" model by means of which we can explain the occurrence of reactions (a) and (b) and their probability according to the most reliable experiments [6]. First of all, we will start by analysing the environment, i.e. of plasmas present within palladium (d-electron, s-electron, Pd-ions and D-ions) using the coherence theory of matter; lastly we will use the effective potential reported in [7,8] adding the role of lattice perturbations by means of which we compute the D–D tunnelling probability.

2. The Plasmas Present within No Loaded Palladium

According to the Coherence Theory of Condensed Matter, in a Pd crystal at room temperature the electron shells are in a coherent regime within coherent domain. In fact they oscillate in tune with a coherent e.m. field trapped in the coherent domains.

So we must take into account the plasma of s-electron and d-electron, in order to describe the lattice environment.

2.1. The Plasma of the d-Electrons

Similar argumentations were proposed by Preparata's but started from a new formulation of condense matter theory known as Coherence Theory.

In this theory, we can visualize the plasma formed by d-shell electrons as consisting of charged shells of charge $n_{\mathrm{d}}e$ (for palladium $n_{\mathrm{d}} = 10$) radius $r_{\mathrm{d}} = 1$ Å and thickness a fraction of 1 Å. The classical plasma

$$\omega_{\mathrm{d}} = \frac{e}{\sqrt{m}}\sqrt{\frac{n_{\mathrm{d}}N}{V}}, \tag{26}$$

as d-electrons plasma frequency. But according to the coherence theory of matter we must adjust this plasma frequency of a factor 1.38.

We can understand this correction by observing that the formula (26) is obtained assuming a uniform d-electron charge distribution. But of course the d-electron plasma is localized in a shell of radius R (that is about 1 Å), so the geometrical contribution is

$$\sqrt{\frac{6}{\pi}} = 1.38. \tag{27}$$

If we rewrite it with ω_{d} the renormalized d-electron plasma frequency, we have

$$\omega_{\mathrm{d}} = 41.5 \text{ eV}/\hbar \tag{28}$$

and the maximum oscillation amplitude ξ_{d} is about 0.5 Å.

2.2. The Plasma of Delocalized s-Electrons

The s-electrons are those which in the lattice neutralize the adsorbed deuterons ions. They are delocalised and their plasma frequency depends on loading ratio (D/Pd percentage). The formula (28) can also be written as

$$\omega_{\mathrm{se}} = \frac{e}{\sqrt{m}}\sqrt{\frac{N}{V}}\sqrt{\frac{x}{\lambda_{\mathrm{a}}}}, \tag{29}$$

where

$$\lambda_a = \left[1 - \frac{N}{V} V_{Pd}\right], \tag{30}$$

and V_{Pd} is the volume effectively occupied by the Pd-atom. As reported in [5], we obtain

$$\omega_{se} \approx x^{1/2} 15.2 \text{ eV}/\hbar. \tag{31}$$

For example for $x = 0.5$, we have $\omega_{se} \sim 10.7 \text{ eV}/\hbar$.

2.3. The Plasma of Pd-ions

Further, we can consider the plasma due to the palladium ions forming the lattice structure; in this case it is possible to demonstrate that the frequency is Eq. (28):

$$\omega_{pd} = 0.1 \text{ eV}. \tag{32}$$

3. The Plasmas Present within D_2-Loaded Palladium

In this section, we seek to show what happens when the absorbed deuterium is placed near to the palladium surface. This loading can be enhanced using electrolytic cells or vacuum chambers working at opportune pressure [9–11]. By means of Preparata's theory of Condensed Matter it is assumed that, according to the ratio x = D/Pd, there are three phases concerning the D_2–Pd system:

(1) Phase α for $x < 0.1$,
(2) Phase β for $0.1 < x < 0.7$,
(3) Phase γ for $x > 0.7$.

In phase α, the D_2 is in a disordered and not coherent state (D_2 is not charged).

According to the other phases, we start remembering that on the surface, because of the lattice e.m., takes place the following reaction:

$$D_{lattice} \to \quad D^+ + e^-. \tag{33}$$

Then, according to the loading quantity x = D/Pd, the ions of deuterium can occur on the octahedral sites (Fig. 1) or on the tetrahedral (Fig. 2) in the (1,0,0)-plane. In the coherent theory of the so called β-plasma of Preparata's the deuterons plasma are in the octahedral site and the γ-plasma are in the tetrahedral.

Regarding to the β-plasma it is possible to affirm that the plasma frequency is given by Eq. (28):

$$\omega_\beta = \omega_{\beta 0}(x + 0.05)^{1/2}, \tag{34}$$

where

$$\omega_{\beta 0} = \frac{e}{\sqrt{m_D}} \left(\frac{N}{V}\right)^{1/2} \frac{1}{\lambda_a^{1/2}} = \frac{0.15}{\lambda_a^{1/2}} \text{eV}/\hbar. \tag{35}$$

For example if we use $\lambda_a = 0.4$ and $x = 0.5$ we obtain $\omega_\beta = 0.168 \, \text{eV}/\hbar$.

In the tetrahedral sites the D^+ can occupy the thin disk that encompass two sites (Fig. 3), representing a barrier to the D^+ ions. We must underline that the electrons of the d-shell start oscillating near to the equilibrium distance y_0 (about 1.4 Å) so that the static ions have a cloud of negative charge (see [5]).

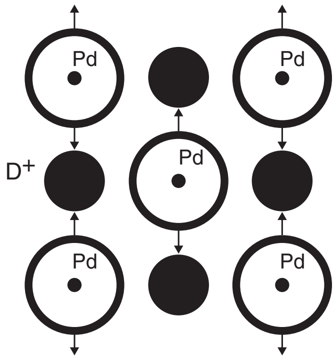

Figure 1. The octahedral sites of the Pd lattice where the deuterons take place.

Then follows:

$$\omega_\gamma = \sqrt{\frac{4Z_{\text{eff}}\alpha}{m_D y_0^2}} \approx 0.65 \text{ eV}/\hbar. \tag{36}$$

Of course this frequency also depends by the chemical condition of the palladium (impurities, temperature, etc…)

Due to a large plasma oscillation of d-electrons, in the disk-like tetrahedral region (where the γ-phase D^+'s are located) condenses a high density negative charge giving rise to a screening potential $W(t)$ whose profile is reported in Fig. 4.

Having mapped that Phase-γ depends on x value other can experimentally observe the new phase in [11,12], very important in the (LERN) investigation. This is demonstrated by the fact that many of the "cold fusion physicist" declare that the main point of cold fusion protocol is the loading D/Pd ratio higher than 0.7, i.e. the deuterium takes place in the tetrahedral sites.

4. The D–D Potential

In [7], it was shown that the phenomenon of fusion between nuclei of deuterium in the lattice of a metal is conditioned by the structural characteristics, by the dynamic conditions of the system and also by the concentration of impurities present in the metal under examination.

In fact, studying the curves of the potential of interaction between deuterons (including the deuteron–plasmon contribution) in the case of three typical metals (Pd, Pt and Ti), as shown in a three-dimensional model, the height of the Coulomb barrier decreases on the varying of the total energy and of the concentration of impurities present in the metal itself.

The initial potential that connects the like-Morse attraction and the like-Coulomb repulsion can be written as seen in [7,8]:

$$V(r) = k_0 \frac{q^2}{r}\left(V(r)_M - \frac{\Sigma}{r}\right), \tag{37}$$

where $V(r)_M$ is the Morse potential, $k_0 = 1/4\pi\varepsilon_0$, q is the charge of the deuteron, M_d the reduced mass of the deuterium nuclei, T the absolute temperature at which the metal is experimentally placed, J the concentration of impurities in the crystalline lattice and R is the nuclear radius.

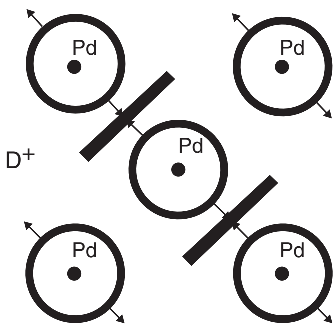

Figure 2. The thin disks of the tetrahedral sites of the Pd lattice where the deuterons take place.

In Eq. (37), $V(r)_{\mathrm{M}}$ is a like-Morse potential, and is given by

$$V(r)_{\mathrm{M}} = B\left\{\exp\left(-2\varphi(-r_0)\right) - 2\exp\left(-\varphi(r - r_0)\right)\right\}. \tag{38}$$

Here the parameters B, φ and r_0 depend by the lattice.

In fact, the potential (37) is an effective one whose reliability is demonstrated by its ability to fit the Coulomb potential for $r \to 0$ and the Morse potential in the attractive zone. So, Siclen and Jones [12] defined ρ the point where the Coulomb potential is associated to the Morse trend, r_0' the equilibrium distance and D' the well.

Of course in the free space for a D_2 molecule, ρ is about 0.3 Å, r_0' is about 0.7 Å and D' is −4.6 eV.

But within the lattice there are the screening effect and the deuteron–deuteron interaction, by means of phonon exchange, modify these parameter values.

Since the screening effect can be modulated by the giver atoms, we have considered in [7,8] the role of impurities and it has been shown that we can write $J = J_0 \exp[\beta/bkT]$.

Further, could occur some particular reactions, incorporating the impurities in the nucleus of the dislocations, as a result of the different arrangement of the atoms with respect to that of the unperturbed lattice.

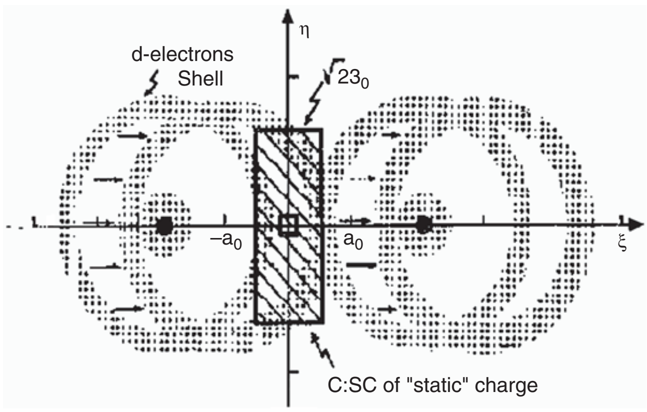

Figure 3. Possible d-electron plasma oscillation in a Pd lattice.

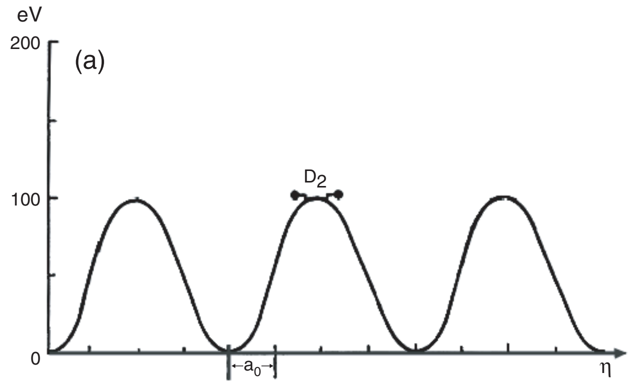

Figure 4. The profile of the electrostatic potential in a arbitrarily direction η.

This type of process has been extensively studied in the literature for metals and for the case of crystalline semiconductors at high temperature.

In the latter, for example, it is found that the concentration of interstitial impurities around a linear dislocation, with a point component, depends on the temperature according to the law written above where J_0 is the concentration of impurities in the zone with zero internal pressure, ($b^3 \simeq v_{\mathrm{i}}$) the volume of the ions constituting the lattice, while β is proportional to the difference ($v_d - v_i$) between the volume of the impurity atoms and that of the lattice ions.

Our conjecture is that in a metal, such as Pd, a similar phenomenon could occur between the atoms of deuterium penetrating the lattice as a result of deuterium loading and the microcracks produced by variations in temperature. In this case, the parameter β of the previous expression would be negative, determining an increase in the concentration of deuterons in the vicinity of the microcrack, which would then catalyse the phenomenon of fusion as:

$$\Sigma = JKTR \tag{39}$$

and

$$B = J/\varsigma.$$

So we can write the effective d–d potential

$$V(r) = k_0 \frac{q^2}{r}\left(V(r)_{\mathrm{M}} - \frac{JKTR}{r}\right), \tag{40}$$

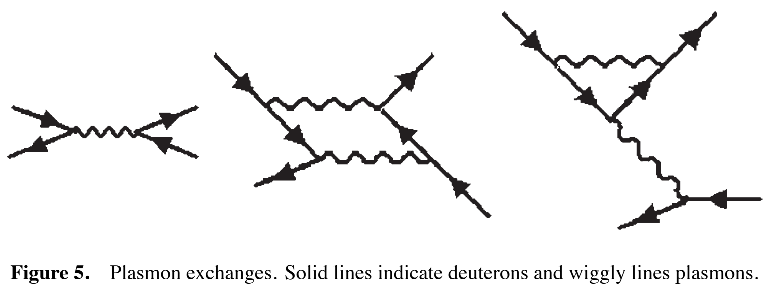

Figure 5. Plasmon exchanges. Solid lines indicate deuterons and wiggly lines plasmons.

where $V(r)_{\mathrm{M}}$ is the Morse potential, $k_0 = 1/4\pi\varepsilon_0$, q is the charge of the deuteron, M_{d} the reduced mass of the deuterium nuclei, T the absolute temperature at which the metal is experimentally placed, J the concentration of impurities in the crystalline lattice and R is the nuclear radius.

Considering the attractive force, due to the exchange of plasmons, the main contribution are those (Fig. 5):

Taking into account the role of coupling between deuteron and plasmons, in [13] it was numerically evaluated a D–D potential having the features of the potential (14) with $D' = -50$ eV and $r_0' = 0.5$ Å and $\rho = 0.2$ Å (remember that in [13] are considered only two plasmon excitations at 7.5 and 26.5 eV).

The feature of the potential (37) is shown in Fig. 6:

According to the coherence theory of condensed matter, we study the role of potential (40) in the three different phases : α, β and γ.

This section, however, needs of some important explanation, such as:

(1) what KT is,;
(2) what is the role of electrons, ions plasma?

Concerning with the first point, according to the different deuteron-lattice configurations, KT can be:

(1) the loaded lattice temperature if we consider the deuterons in the α-phase;
(2) ω_β if we consider the deuterons in β-phase;
(3) ω_γ if we consider the deuterons in the γ-phase;

The question is much more complicate for the second point. In fact the lattice environment is a combination of coherent plasmas (ion Pd, electron and deuterons plasma) at different temperature, due to different masses, that let be very difficult the description of the emerging potential.

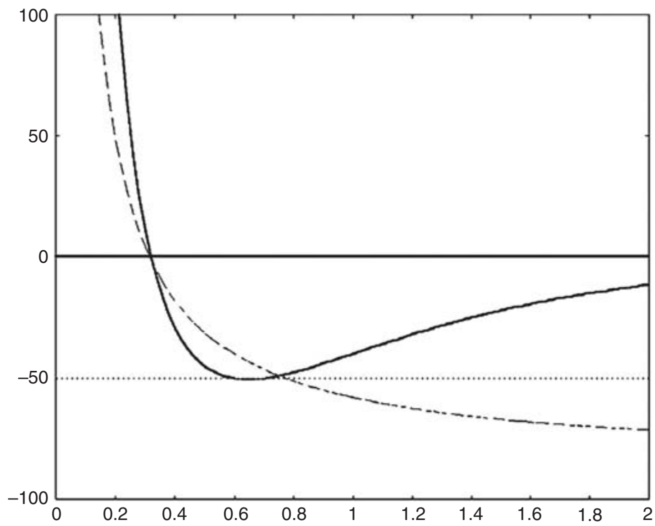

Figure 6. The solid line shows the features of potential (37) computed in order to obtain $D' = -50$ eV and $\rho = 0.165$ Å. The Coulomb potential in dashed line is computed using a screening constant of 85 eV. In the x-axis is reported the distance in Bohr radius unit and on the y-axis the energy in eV.

The method that in this work we propose is the following: to consider the total screening contribution of lattice environment at D–D interaction (i.e. V_{tot}) as random potential $Q(t)$. So in this model we have

$$V_{\mathrm{tot}}(t) = V(r) + Q(t). \tag{41}$$

Of course we assume that

$$\langle Q(t)\rangle_t \neq 0 \tag{42}$$

that is to say that $Q(t)$ (a second order potential contribution) is a periodic potential (the frequency will be called by ω_Q) that oscillates between the maximum value $Q_{\max}$ and 0.

More exactly the oscillation charges of *d-shell* produce a screening potential having a harmonic feature:

$$eV(r) = -Z_{\mathrm{d}}\frac{ke^2}{2a_0}r^2. \tag{43}$$

In [5] putting $Z_{\mathrm{d}} = 10/3$ and $a_0 = 0.7$ Å, it is evaluated a screening potential V_0 of about 85 eV. In this way we can compute $\rho = V_0/26.9$ and at last $\rho = 0.165$ Å. To summarize, we can have the following cases in a palladium lattice according to the loading ratio:

4.1. α-Phase

In the phase α the deuterons are in a molecular state and the thermal motion is about:

$$0.02 \text{ eV} < \hbar\omega_\alpha < 0.1 \text{ eV}.$$

This phase takes places when x is fewer than 0.1, and since $W(t)$ is zero, the D–D potential is

$$V(r) = k\frac{q^2}{r}\left(V_{\mathrm{M}}(r) - \frac{J\hbar\omega_\alpha R}{r}\right). \tag{44}$$

The expression (44) was partially evaluated in the previous paper [7]; in fact, we were only interested in the dependence of the tunnelling probability on impurities present within lattice. Through this work, we seek to examine the correlation between potential features and loading ratio and in the paragraph 5 we showed some numerical results.

4.2. β-Phase

When x is bigger than 0.1 but fewer than 0.7, the phase-β happens. The interaction takes place among deuteron ions that oscillate between the following energy values:

$$0.1 \text{ eV} < h\omega_\beta < 0.2 \text{ eV}.$$

In this case $W(t)$ is zero, we give this expression to the potential

$$V(r) = k\frac{q^2}{r}\left(V_{\mathrm{M}}(r) - \frac{J\hbar\omega_\beta R}{r}\right). \tag{45}$$

Comparing the expressions (44) and (45), it seems clear that the weight of impurities is more important in the β-phase. Of course, this conclusion deals with the previous papers [7,8] in which we studied the role of temperature on tunnelling effect.

Table 1. For Pd "Impure" ($J \approx 0.75\%$), using the α-phase potential (44), has been computed the fusion probability normalized to the number of event/s for different values of energy (-50 eV $<$ E $<$ 50 eV) (Palladium $J \approx 0.75\%$, $\rho \approx 0.34$ Å, $r'_0 = 0.7$ Å, $D' = -50$ eV)

$\omega_\alpha \approx 0.0025$ eV	$\omega_\alpha \approx 0.05$ eV	$\omega_\alpha \approx 0.075$ eV	$\omega_\alpha \approx 0.1$ eV
$E \approx -50$, $P \approx 10^{-100}$	$E \approx -50$, $P \approx 10^{-103}$	$E \approx -50$, $P \approx 10^{-100}$	$E \approx -50$, $P \approx 10^{-99}$
$E \approx -40$, $P \approx 10^{-99}$	$E \approx -40$, $P \approx 10^{-101}$	$E \approx -40$, $P \approx 10^{-98}$	$E \approx -40$, $P \approx 10^{-97}$
$E \approx -30$, $P \approx 10^{-97}$	$E \approx -30$, $P \approx 10^{-100}$	$E \approx -30$, $P \approx 10^{-96}$	$E \approx -30$, $P \approx 10^{-96}$
$E \approx -20$, $P \approx 10^{-95}$	$E \approx -20$, $P \approx 10^{-99}$	$E \approx -20$, $P \approx 10^{-94}$	$E \approx -20$, $P \approx 10^{-93}$
$E \approx -10$, $P \approx 10^{-94}$	$E \approx -10$, $P \approx 10^{-97}$	$E \approx -10$, $P \approx 10^{-91}$	$E \approx -10$, $P \approx 10^{-90}$
$E \approx 0$, $P \approx 10^{-92}$	$E \approx 0$, $P \approx 10^{-96}$	$E \approx 0$, $P \approx 10^{-90}$	$E \approx 0$, $P \approx 10^{-86}$
$E \approx 10$, $P \approx 10^{-91}$	$E \approx 10$, $P \approx 10^{-94}$	$E \approx 10$, $P \approx 10^{-87}$	$E \approx 10$, $P \approx 10^{-83}$
$E \approx 20$, $P \approx 10^{-90}$	$E \approx 20$, $P \approx 10^{-92}$	$E \approx 20$, $P \approx 10^{-85}$	$E \approx 20$, $P \approx 10^{-80}$
$E \approx 30$, $P \approx 10^{-89}$	$E \approx 30$, $P \approx 10^{-90}$	$E \approx 30$, $P \approx 10^{-82}$	$E \approx 30$, $P \approx 10^{-78}$
$E \approx 40$, $P \approx 10^{-86}$	$E \approx 40$, $P \approx 10^{-89}$	$E \approx 40$, $P \approx 10^{-80}$	$E \approx 40$, $P \approx 10^{-74}$
$E \approx 50$, $P \approx 10^{-84}$	$E \approx 50$, $P \approx 10^{-87}$	$E \approx 50$, $P \approx 10^{-79}$	$E \approx 50$, $P \approx 10^{-71}$

4.3. γ-Phase

Lastly, when the loading ratio is higher than 0.7, the deuteron–palladium system is in the phase-γ.

This is the most interesting case. The deuterons cross the screening through the d-electrons shell, in this sense we did a numeric simulation where we suppose that the D–D potential must be computed assuming that the well present in potential (37), because of the Morse contribution, disappears. In fact if we use a classical plasma model where the D^+ ions are the positive charge and the d-electrons the negative one, it is very "realistic" to use the following potential:

$$V(r,t) = k\frac{q^2}{r}\left(V_M(r) - \frac{J\hbar\omega_\gamma R}{r}\right) + Q(t), \tag{46}$$

where $Q(t)$ is a not known perturbative potential. About this we can also add that

$$\langle Q(t)\rangle_t \approx \frac{W_{\max}}{\sqrt{2}}. \tag{47}$$

As said previously, we suppose that it is the screening potential, because of the d-electrons, has the role to reduce the repulsive barrier, i.e. ρ and r'_0. In the next evaluation it is given

$$\langle Q(t)\rangle_t \approx 85 \text{ eV}. \tag{48}$$

5. Conclusion

The aim of this section is to present the D–D fusion probability normalized to number of events per second regarding the D–D interaction in all different phases. More exactly, we seek to compare, at the varying of energy between –50 and 50 eV, the fusion probability in the phases α, β and γ. We also consider the role of d-electrons screening as perturbative lattice potential.

This treatment, which only interests the case where $Q(t)$ is different from zero, involves the change of the value of the point on the x-axis where the Coulomb barrier takes place; in this case, the final result is that the screening enhances the fusion probability. In order to evaluate the fusion rate (Λ) we applied this formula:

$$\Lambda = A\Gamma, \tag{50}$$

Table 2. For Pd "Impure" ($J \approx 0.75\%$), using the β-potential (45), has been computed the fusion probability P normalized to the number of event/s for different values energy (-50 eV $< E <$ 50 eV) (Palladium $J \approx 0.75\%, \alpha \approx 0.34$ Å, $r'_0 = 0.7$ Å, $D' = -50$ eV)

$\omega_\beta \approx 0.125$ eV	$\omega_\beta \approx 0.150$ eV	$\omega_\beta \approx 0.175$ eV	$\omega_\beta \approx 0.2$ eV
$E \approx -50, P \approx 10^{-83}$	$E \approx -50, P \approx 10^{-88}$	$E \approx -50, P \approx 10^{-86}$	$E \approx -50, P \approx 10^{-81}$
$E \approx -40, P \approx 10^{-81}$	$E \approx -40, P \approx 10^{-87}$	$E \approx -40, P \approx 10^{-85}$	$E \approx -40, P \approx 10^{-75}$
$E \approx -30, P \approx 10^{-80}$	$E \approx -30, P \approx 10^{-86}$	$E \approx -30, P \approx 10^{-83}$	$E \approx -30, P \approx 10^{-73}$
$E \approx -20, P \approx 10^{-79}$	$E \approx -20, P \approx 10^{-85}$	$E \approx -20, P \approx 10^{-80}$	$E \approx -20, P \approx 10^{-70}$
$E \approx -10, P \approx 10^{-78}$	$E \approx -10, P \approx 10^{-84}$	$E \approx -10, P \approx 10^{-74}$	$E \approx -10, P \approx 10^{-68}$
$E \approx 0, P \approx 10^{-76}$	$E \approx 0, P \approx 10^{-82}$	$E \approx 0, P \approx 10^{-73}$	$E \approx 0, P \approx 10^{-62}$
$E \approx 10, P \approx 10^{-75}$	$E \approx 10, P \approx 10^{-81}$	$E \approx 10, P \approx 10^{-72}$	$E \approx 10, P \approx 10^{-60}$
$E \approx 20, P \approx 10^{-74}$	$E \approx 20, P \approx 10^{-79}$	$E \approx 20, P \approx 10^{-71}$	$E \approx 20, P \approx 10^{-54}$
$E \approx 30, P \approx 10^{-73}$	$E \approx 30, P \approx 10^{-76}$	$E \approx 30, P \approx 10^{-70}$	$E \approx 30, P \approx 10^{-50}$
$E \approx 40, P \approx 10^{-72}$	$E \approx 40, P \approx 10^{-75}$	$E \approx 40, P \approx 10^{-69}$	$E \approx 40, P \approx 10^{-45}$
$E \approx 50, P \approx 10^{-71}$	$E \approx 50, P \approx 10^{-70}$	$E \approx 50, P \approx 10^{-65}$	$E \approx 50, P \approx 10^{-42}$

where Γ the Gamow factor and A is the nuclear reaction constant obtained from measured cross sections (value used was 10^{22} s^{-1}).

From an experimental point of view, in the cold fusion phenomenology, it is possible to affirm that there are three typologies of experiments [14]:

(1) those giving negative results,
(2) those giving some results (little detection signs with respect to background, fusion probability about 10^{-23} using a very high loading ratio),
(3) those giving clear positive results such as the Fleischmann and Pons experiments.

Nevertheless, we think that from the experimental point of view, the experiments of the third point are few accurate. In this sense, we believe that a theoretical model of controversial phenomenon of cold fusion is better to explain only those experiments of the points 1 and 2. In this case, it is important to consider the role of loading ratio on the experimental results. Now, let us begin from the α-phase.

In Table 1 are shown the results about the α-phase. Here we can observe that the theoretical fusion probability is very low, fewer than 10^{-74}. Consequently, it is allowed to affirm that through the loading, in the deuterium, of a percentage of $x < 0.2$ it is not possible any fusion. The same absence of nuclear phenomenon is compatible for a loading ratio of about 0.7 (Table 2) since in this case the predicted fusion probability is fewer than 10^{-42}. These predictions, of course, agree with the experimental results (for $x > 0.7$ look at [6]). The result of our model is that in the γ-phase, where we can observe some background fluctuations in which, because of a high loading ratio, we predict a fusion probability at about 10^{-22}. This is a new result, very important for [7,8] since, in those cases, the fusion probability was independent from the loading ratio.

To conclude, our aim is also to show that the model proposed in this paper (which unify nuclear physics with condensed matter) can explain some irregular nuclear traces in the solids. Regarding the experiments at point 3, on the other hand, supposing that those could be real, we want to consider other contributions as microdeformation occurrence in order to explain the very high fusion rate. The role of microcrack and impurities linked by loading ratio will be explored in other speculative works. "The nuclear physics within condensed matter" may be a new device through which it is possible to understand other new productive scientific topic.

The studied problem is the objective of proposing a theoretical model considering the *random city* of the phenomenon and that permits to those experiments (in which there is a high production of energy) to be repetitive and reproductive.

Table 3. For Pd "Impure" ($J \approx 0.75\%$), using the γ-potential (46), has been computed the fusion probability normalized to the number of event/s for different values of energy (-50 eV $< E <$ 50 eV) (Palladium $J \approx 0.75\%$, $\rho \approx 0.165$ Å, $r'_0 = 0.35$ Å, $D' = -50$ eV)

$\omega_\gamma \approx 0.6$ eV	$\omega_\gamma \approx 0.65$ eV	$\omega_\gamma \approx 0.7$ eV	$\omega_\gamma \approx 0.75$ eV
$E \approx -50$, $P \approx 10^{-71}$	$E \approx -50$, $P \approx 10^{-51}$	$E \approx -50$, $P \approx 10^{-57}$	$E \approx -50$, $P \approx 10^{-50}$
$E \approx -40$, $P \approx 10^{-68}$	$E \approx -40$, $P \approx 10^{-49}$	$E \approx -40$, $P \approx 10^{-54}$	$E \approx -40$, $P \approx 10^{-47}$
$E \approx -30$, $P \approx 10^{-66}$	$E \approx -30$, $P \approx 10^{-47}$	$E \approx -30$, $P \approx 10^{-51}$	$E \approx -30$, $P \approx 10^{-44}$
$E \approx -20$, $P \approx 10^{-62}$	$E \approx -20$, $P \approx 10^{-44}$	$E \approx -20$, $P \approx 10^{-49}$	$E \approx -20$, $P \approx 10^{-41}$
$E \approx -10$, $P \approx 10^{-60}$	$E \approx -10$, $P \approx 10^{-41}$	$E \approx -10$, $P \approx 10^{-46}$	$E \approx -10$, $P \approx 10^{-39}$
$E \approx 0$, $P \approx 10^{-57}$	$E \approx 0$, $P \approx 10^{-39}$	$E \approx 0$, $P \approx 10^{-43}$	$E \approx 0$, $P \approx 10^{-36}$
$E \approx 10$, $P \approx 10^{-54}$	$E \approx 10$, $P \approx 10^{-38}$	$E \approx 10$, $P \approx 10^{-42}$	$E \approx 10$, $P \approx 10^{-33}$
$E \approx 20$, $P \approx 10^{-51}$	$E \approx 20$, $P \approx 10^{-35}$	$E \approx 20$, $P \approx 10^{-40}$	$E \approx 20$, $P \approx 10^{-32}$
$E \approx 30$, $P \approx 10^{-49}$	$E \approx 30$, $P \approx 10^{-32}$	$E \approx 30$, $P \approx 10^{-36}$	$E \approx 30$, $P \approx 10^{-29}$
$E \approx 40$, $P \approx 10^{-47}$	$E \approx 40$, $P \approx 10^{-30}$	$E \approx 40$, $P \approx 10^{-33}$	$E \approx 40$, $P \approx 10^{-25}$
$E \approx 50$, $P \approx 10^{-45}$	$E \approx 50$, $P \approx 10^{-27}$	$E \approx 50$, $P \approx 10^{-30}$	$E \approx 50$, $P \approx 10^{-21}$

Our starting point is the following: the phenomenon of the low-energy fusion critically, depends on the interaction between the d-d nuclear system and the D_2 gas system, and the lattice of the palladium.

In fact, at the variation of the loading percentage, the typical deuterium–plasma interaction of the γ phase grows up and so the electrostatic repulsion is weakened. But while the deuterium loading in the gas phase grows up, the palladium lattice is deformed.

Other theoretical and experimental studies about the electric field are in progress. In order to be more clear, we explain the main passages of the lattice reaction: firstly, we have the deformation; secondly, the dislocation; and lastly the microcrack.

If the lattice is deformed, within the microcrack one has the creation of a microscopic electric field, in which the D^+ and the plasmons come to collision, and in which the deuterium nuclei are accelerated, as it happens in a classic accelerator of nuclear physic. This acceleration can also generate the phenomenon of the low-energy fusion.

References

[1] Y. Iwamura et al., *Jpn. J. Appl. Phys. A* **41** (1994) 4642.
[2] O. Reifenschweiler, *Phys. Lett. A* **184** (1994) 149.
[3] O. Reifenschweiler, *Fusion Technol.* **30** (1996) 261.
[4] H. Melvin Miles et al., *Fusion Technol.* **25** (1994) 478.
[5] G. Preparata, *QED Coherence in Matter* (World Scientific Publishing, Singapore, 1995).
[6] S. Aiello et al., *Fusion Technol.* **18** (1990) 125.
[7] F. Frisone, *Fusion Technol.* **39** (2001) 260.
[8] F. Frisone, *Fusion Technol.* **40** (2001) 139.
[9] F. Fleishmann and Pons, *J. Electroanal. Chem.* **261** (1989) 301–308.
[10] A. De Ninno et al., *Europhys. Lett.* **9** (1989) 221–224.
[11] G. Mengoli et al., *J. Electroanal. Chem.* **350** (1989) 57.
[12] C. DeW Van Siclen, S.E. Jones, *J. Phys.G. Nucl. Phys.* **12** (1986).
[13] M. Baldo, R. Pucci, *Fusion Technol.* **18** (1990) 47.
[14] D.R.O. Morrison, Review of cold fusion, *in Eighth World Hydrogen Energy Conference*, 1990, Honolulu, Hawaii Natural Energy Institute, Honolulu, HI.

J. Condensed Matter Nucl. Sci. 1 (2007) 41–46

Research Article

Calculation of Deuteron Interactions within Microcracks of a D_2 Loaded Crystalline Lattice at Room Temperature

Frisone Fulvio*

Department of Physics, University of Catania, Via Santa Sofia 64, I-95125 Catania, Italy

Abstract

We have analysed the possibility that the coefficient of lattice deformation, linked to the formation of microcracks at room temperature and low energies, could influence the process of fusion. The calculated probability of fusion within a microcrack, in the presence of D_2 loading at room temperature and for impure metals, shows moderately elevated values compared with the probability of fusion on the surface. For all the temperatures in the 150–350 K range and for all the energies between 150 and 250 eV, the formation of microcracks increases the probability of fusion compared to non-deformed lattices, and also reduces the thickness of the Coulomb barrier. Using the trend of the curve of potential to evaluate the influence of the concentration of impurities, a very high barrier is found within the pure lattice ($J \approx 0.25\%$). However, under the same thermodynamic conditions, the probability of fusion in the impure metal ($J \approx 0.75\%$) could be higher, with a total energy less than the potential so that the tunneling effect is amplified. Finally, we analysed the influence of *forced* D_2 loading on the process.

Keywords: Collective plasmonic excitation, Dislocations, Fusion within a microcrack, Tunneling effect

1. Introduction

This study has the aim of analyzing the possible influence, which variations in temperature and energy could have on the phenomenon of deuterium fusion because of microdeformations or microcracks produced in the lattice. These could in fact be able to concentrate in their vicinity a significant fraction of the deuterons present in the metal. In particular, the author has suggested [1] that deuteron–plasmon coupling could increase the rate of fusion by acting as an effective interaction attractive to deuterium nuclei, reducing the distance at which Coulomb repulsion becomes dominant. With this in mind, a study was made of crystalline lattices with certain structural characteristics: in particular, the analysis focused on lattices with ten or more electrons in the "d" band. The present work will concentrate on palladium because, when subjected to thermodynamic stress, this metal has been seen to give results which are interesting from both the theoretical and experimental points of view.

*E-mail: Frisone@ct.infn.it

Further, it is hypothesized that the phenomenon of fusion is not only conditioned by structural characteristics and the thermodynamic conditions of the system, but also by the concentration of impurities present in the metal, correlated with the deuterium loading within the lattice itself.
The analysis will attempt to determine whether, in the case of the three-dimensional isotrope, D_2 loading can lead to the formation of microcracks in an analogous manner to that suggested for temperature variation in [1]. This would constitute an ulterior verification of the hypotheses proposed.

2. Three-dimensional Model

The aim is to determine whether, and within what limits, deuterium loading can condition the rate of fusion within a generic cubic lattice, trying to isolate the D_2 contribution from any other possible effects caused by lattice defects, or by other characteristics or thermodynamic conditions, or even by any "microdeformations" of the crystalline lattice caused by temperature variations. This type of phenomenon can be considered as a perturbation "external" to the system [2] and should be distinguished from "internal" perturbations.

In the case of external perturbations, the interaction between the impurities present and the dislocations [4] produced in the metal during microdeformation can distinctly modify the electrical properties of the material. Because of the different arrangement of the atoms with respect to the unperturbed lattice, some particular reactions can then occur so that the impurities become incorporated in the nucleus of the dislocations.

The results presented here were obtained using a numerical simulation to determine the trend of the barrier penetration factor, K, as a function of the temperature and the concentration of impurities present in the metal under examination.

In a three-dimensional model, the probability of fusion between not-free deuterium nuclei within the crystalline lattice is equal to the probability of penetrating a Coulomb potential barrier $V(r)$, given by

$$|P|^2_{\mathrm{int}} = \exp\left(2\int_0^{\alpha} K\,(r)_{\mathrm{int}}\,\mathrm{d}r\right), \tag{1}$$

where α is 0.11 Å and $K(r)_{\mathrm{int}}$ is given by

$$K\,(r)_{\mathrm{int}} = \sqrt{2\mu\,[E - V\,(r)]\,/\hbar^2} \tag{2}$$

E is the initial total energy (in eV), principally thermal in nature; μ is reduced mass of the deuteron and $\hbar$ is the Plank's constant.

The interaction potential can then be further extended to the three-dimensional isotrope case.

The potential $V(r)_{\mathrm{int}}$ will then be expressed in the following way:

$$V\,(r)_{\mathrm{int}} = k\frac{q^2}{r}\left[V\,(r)_{\mathrm{M}} - J\frac{\xi kTR}{r}\right], \tag{3}$$

where $k = 1/4\pi\varepsilon_0$, q is the deuteron charge, R the nuclear radius, ξ a parameter which depends on the structural characteristics of the lattice (number of "d" band electrons and type of lattice symmetry), varying between 0.015 and 0.025, T the absolute temperature of the metal under experimental conditions and J is the percentage of impurities in the crystalline lattice.

In this case the Morse potential will be:

$$V(r)_{\mathrm{M}} = (J/\varsigma)\,\exp\left(-2\varphi\,(r - r_0)\right) - 2\exp\left(-\varphi\,(r - r_0)\right). \tag{4}$$

In this equation, the parameters ς and φ depend on the dynamic conditions of the system, while r_0 is the classic point of inversion.

Equations (1) and (2) refer to the process of "not free" fusion, i.e. fusion within the crystalline lattice.

The "catalyzing" effect of the lattice has been studied from the theoretical point of view: in particular, it was shown [1] that, considering the interaction between deuterium nuclei and collective plasmonic excitation in the metal, fusion rate λ_f in a gas consisting of λ deuterons with densityρ is given by

$$\lambda_f = \lambda \frac{4\pi\rho\hbar}{\mu_d} \langle 1/p \rangle , \tag{5}$$

where μ_d is the mass of the deuterium nuclei, p is their impulse, and where the parentheses $\langle\rangle$ represent the thermal mean.

The aim of this work is to demonstrate the possibility of a further effect enhancing the probability of fusion, principally due to the presence of impurities in the metal.

The effect of vibrational energy, which is typically of the order of some eV for the quantum states under consideration, will be ignored here.

Electronic screening, a result of the metallic lattice, represents an important effect on the fusion reaction. Already studied by Rabinowitz et al. [3], this effect can be taken into account using a model in which the negative charge is distributed over a thin shell of radius R.

Because of the interaction potential within the metal, the "shifted" Coulomb potential can be written as:

$$V = kq^2 [(1/r) - (1/R)] , \quad r_1 \leq r \leq R, \tag{6}$$

where q is the charge of the deuteron, r_1 is the nuclear radius and $k = 1/4\pi\varepsilon_0$.

This gives $V = 0$ per $r > R$.

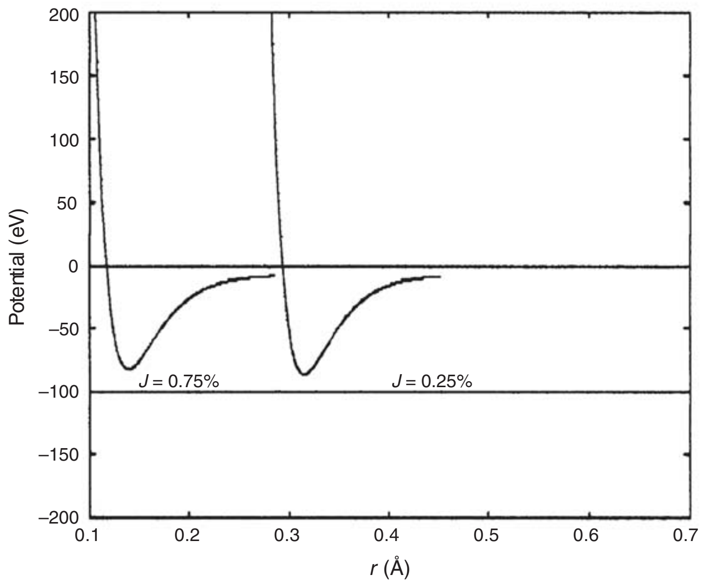

Figure 1. Semi-classic tunneling appears increased for those metals that have a concentration of impurity $J \approx 0.75\%$. The Morse potential was calculated at $T = 290$ K. The Coulomb barrier seems very high in the case of pure metals with $J \approx 0.25\%$. The "shell" potential was calculated at $T = 290$ K.

The solution for the semi-classic tunneling factor Λ is [3]:

$$\Lambda = D \exp\{-2\gamma(r_1)\}, \tag{7}$$

$$\gamma(r_1) = (\pi/2\hbar)\left[(2q^2/4\pi\varepsilon_0)\mu r_2\right]^{1/2}. \tag{8}$$

In Eq. (7), D is a numerical constant of the order of unity, μ the effective reduced mass of the deuteron, r_2 the classical turning point of d–d Coulomb collision process and $\hbar$ is the Plank's constant. To take into account the effect of the impurities present, the product $J\eta$ is substituted for D in Eq. (7), where J represents the concentration of impurities and η is a numerical constant.

It is now possible to consider a cubic lattice structure subjected to microdeformations and calculate the probability of fusion within a microcrack, Γ, on varying the temperature.

Indicating the volume of a single cell by $\mathrm{d}\Omega$, the deformation of the entire lattice is given by

$$D_{\mathrm{L}} = \iiint_{\omega} J \frac{\rho l^2 \nu b^2}{\alpha 2hR} \exp\left(-\frac{U_0}{kT}\right) \mathrm{d}\omega, \tag{9}$$

where ρ is the density of the mobile dislocation within the lattice at a non-constant lattice temperature, l^2 the area between the lines of separation between two adjacent dislocations, caused by a curving of the lattice [4], R is a coefficient whose value depends on the stress within the lattice, α is proportional to the thermal increment and represents the effect of the sudden variations in temperature to which the lattice is subjected and which lead to the formation of microcracks, ν^2 is the vibration frequency of the deuterons in the metal, considered constant here, b^2 the stress line which dampens the transformation of the crystalline lattice and $U_0 = 2U_j - Dbd\,(\sigma - \sigma_i)_{\varepsilon_0}$ is the activation energy.

In this last expression, $\sigma - \sigma_i$ is the stress applied to the small dislocations to a good approximation $\sigma_i \simeq \mu b/2\pi\ell$ and ℓ has the dimensions of a wavelength, while μ is an elastic constant which depends on the characteristics of the lattice. $\varepsilon_0 = \varepsilon_\beta - \beta t^m$ where β depends on the temperature and m is a variable which depends on the lattice (in this case it is equal to 1/3). $2U_j \simeq kT_{\mathrm{c}} \ln(X/\dot{\varepsilon})$ is obtained from the comparison of two curves with deformation velocity

Table 1. For "impure" Pd $J \approx 0.75\%$, using the Morse potential, the probability of fusion Γwithin a microcrack in the presence of D_2 loading, normalized to the number of events per minute, was calculated for different values of temperature (varying from 100 to 300 K) and energy (varying from 150 to 250 eV). It should be noted that the probability generally increases with T and E, and is systematically several orders greater than the probability of surface fusion P (Palladium $J \approx 0.75\%$, T(range) $\approx$ 100–300 K, $\alpha \approx 0.34$ Å, $\lambda = 10^{-3}$ eV/min, M_{Pd}/μg)

E (eV)	$T \approx 100$ K		$T \approx 140$ K		$T \approx 180$ K		$T \approx 220$ K		$T \approx 260$ K		$T \approx 300$ K	
	$\Gamma \approx$	$P \approx$	$\Gamma \approx$	$P \approx$	$\Gamma \approx$	$P \approx$	$\Gamma \approx$	$P \approx$	$\Gamma \approx$	$P \approx$	$\Gamma \approx$	$P \approx$
150	10^{-80}	10^{-88}	10^{-67}	10^{-69}	10^{-77}	10^{-86}	10^{-63}	10^{-65}	10^{-65}	10^{-66}	10^{-60}	10^{-68}
160	10^{-75}	10^{-86}	10^{-65}	10^{-68}	10^{-75}	10^{-85}	10^{-61}	10^{-63}	10^{-63}	10^{-65}	10^{-58}	10^{-65}
170	10^{-72}	10^{-85}	10^{-63}	10^{-65}	10^{-73}	10^{-85}	10^{-60}	10^{-62}	10^{-60}	10^{-64}	10^{-56}	10^{-62}
180	10^{-69}	10^{-83}	10^{-60}	10^{-62}	10^{-72}	10^{-84}	10^{-59}	10^{-61}	10^{-58}	10^{-63}	10^{-55}	10^{-60}
190	10^{-67}	10^{-81}	10^{-57}	10^{-60}	10^{-71}	10^{-83}	10^{-57}	10^{-60}	10^{-56}	10^{-62}	10^{-50}	10^{-58}
200	10^{-66}	10^{-79}	10^{-55}	10^{-59}	10^{-70}	10^{-82}	10^{-55}	10^{-59}	10^{-54}	10^{-61}	10^{-48}	10^{-54}
210	10^{-65}	10^{-76}	10^{-54}	10^{-58}	10^{-69}	10^{-78}	10^{-53}	10^{-57}	10^{-53}	10^{-60}	10^{-47}	10^{-52}
220	10^{-63}	10^{-75}	10^{-52}	10^{-57}	10^{-64}	10^{-77}	10^{-52}	10^{-56}	10^{-52}	10^{-59}	10^{-46}	10^{-51}
230	10^{-60}	10^{-72}	10^{-51}	10^{-56}	10^{-63}	10^{-76}	10^{-51}	10^{-55}	10^{-50}	10^{-58}	10^{-45}	10^{-50}
240	10^{-59}	10^{-67}	10^{-50}	10^{-55}	10^{-62}	10^{-74}	10^{-49}	10^{-54}	10^{-49}	10^{-57}	10^{-43}	10^{-48}
250	10^{-58}	10^{-63}	10^{-49}	10^{-53}	10^{-61}	10^{-72}	10^{-48}	10^{-52}	10^{-48}	10^{-53}	10^{-41}	10^{-46}

$\dot{\varepsilon}$, T_c is the "critical temperature" for the formation of the microcracks and $X \simeq 10^5$ in the CGS system. d indicates the distance between dislocations which have not undergone internal splitting, b can be associated with the inter-atomic distance and D depends on the time of movement of the dislocations. The aim here is to determine the probability of fusion within a deuterium loaded metal.

Further, the same problem will be treated from the aspect of the concentration of impurities contained in the metal.

If Eq. (1) is divided by Eq. (5) and multiplied by Eq. (9), it follows that

$$\Gamma \approx \frac{\exp\left(-2\displaystyle\int_0^{\alpha} K(r)_{\mathrm{int}}\mathrm{d}r\right)}{\lambda \frac{4\pi\rho\hbar}{\mu_{\mathrm{d}}}\langle 1/p\rangle} D_{\mathrm{L}}. \tag{10}$$

Equation (10) represents the probability of deuteron fusion within a microcrack: it is inversely proportional to the number of nuclei absorbed by the metal.

Using Eq. (10) and adopting the Morse potential to calculate $K(r)_{\mathrm{int}}$, the probability of fusion, normalized to the number of events per minute, was obtained by means of a numerical simulation program which utilizes the "WKB" method. The results are reported in Table 1. Within the metal, the probability of fusion given by Eq. (1) was evaluated numerically, making use of Eqs. (3) and (4) and taking the center of mass system as the reference system [1]. In the particular case of impure palladium with:

$$\alpha \simeq 0.15\,\text{Å},\ E \approx 237.2\ \text{eV},\ J = 0.75\%,\ T\ =\ 250.2\,\text{K}.$$

The result is $\Gamma_{\mathrm{pd}} \approx 10^{-41}$, $P_{\mathrm{int}} \approx 10^{-46}$.

For this result, and also for those obtained using the WKB method incorporated in numerical simulation programs, a range of temperatures between 100 and 300 K were considered.

The potential, Eq. (3), for Pd pure to 0.25%, was substituted by the "shell" potential, as follows:

$$V = kq^2\left((1/r) - \frac{KT}{J\varepsilon R}\right), \qquad r_1 \le r \le R, \tag{11}$$

Table 2. For "pure" Pd ($J \approx 0.25\%$), adopting the "shell" potential, the probability of fusion Γwithin a microcrack, normalized to the number of events per minute, was calculated under the same dynamic conditions as in Table 1. Also here $\Gamma$is systematically several orders of magnitude greater than the probability of fusion on the surface P, but the values are systematically lower than those of the previous case (Palladium $J \approx 0.25\%$, $T(\text{range}) \approx 100$–$300\,\text{K}$, $\alpha \approx 0.34\,\text{Å}$, $\lambda = 10^{-3}$ eV/min, $M_{\mathrm{Pd}}/\mu\text{g}$)

E (eV)	$T \approx 100$ K		$T \approx 140$ K		$T \approx 180$ K		$T \approx 220$ K		$T \approx 260$ K		$T \approx 300$ K	
	$\Gamma \approx$	$P \approx$	$\Gamma \approx$	$P \approx$	$\Gamma \approx$	$P \approx$	$\Gamma \approx$	$P \approx$	$\Gamma \approx$	$P \approx$	$\Gamma \approx$	$P \approx$
150	10^{-75}	10^{-81}	10^{-76}	10^{-85}	10^{-73}	10^{-78}	10^{-69}	10^{-75}	10^{-66}	10^{-76}	10^{-65}	10^{-71}
160	10^{-74}	10^{-79}	10^{-78}	10^{-83}	10^{-70}	10^{-77}	10^{-68}	10^{-74}	10^{-65}	10^{-75}	10^{-63}	10^{-70}
170	10^{-73}	10^{-76}	10^{-76}	10^{-81}	10^{-69}	10^{-76}	10^{-67}	10^{-73}	10^{-63}	10^{-74}	10^{-60}	10^{-66}
180	10^{-71}	10^{-75}	10^{-75}	10^{-80}	10^{-68}	10^{-75}	10^{-65}	10^{-72}	10^{-62}	10^{-73}	10^{-58}	10^{-65}
190	10^{-69}	10^{-73}	10^{-73}	10^{-78}	10^{-67}	10^{-74}	10^{-64}	10^{-70}	10^{-60}	10^{-72}	10^{-57}	10^{-64}
200	10^{-67}	10^{-72}	10^{-72}	10^{-75}	10^{-65}	10^{-73}	10^{-62}	10^{-69}	10^{-58}	10^{-71}	10^{-56}	10^{-62}
210	10^{-65}	10^{-70}	10^{-67}	10^{-74}	10^{-64}	10^{-72}	10^{-60}	10^{-68}	10^{-56}	10^{-68}	10^{-55}	10^{-59}
220	10^{-64}	10^{-67}	10^{-68}	10^{-73}	10^{-63}	10^{-70}	10^{-59}	10^{-67}	10^{-54}	10^{-67}	10^{-54}	10^{-57}
230	10^{-63}	10^{-65}	10^{-66}	10^{-71}	10^{-61}	10^{-69}	10^{-57}	10^{-66}	10^{-52}	10^{-65}	10^{-50}	10^{-54}
240	10^{-61}	10^{-63}	10^{-64}	10^{-70}	10^{-60}	10^{-68}	10^{-55}	10^{-64}	10^{-51}	10^{-61}	10^{-49}	10^{-51}
250	10^{-60}	10^{-61}	10^{-63}	10^{-68}	10^{-58}	10^{-64}	10^{-54}	10^{-62}	10^{-49}	10^{-59}	10^{-45}	10^{-48}

dove KT is the mean kinetic energy of the gas, ε is the vibrational energy (typically of the order of some eV for the quantum states considered) and q is the deuteron charge. Under these particular dynamic conditions, the probability of fusion normalized to a number of events per minute was obtained for palladium. The probability of fusion within "pure" palladium, under the same dynamic conditions as the previous example, is then given by:

$$\alpha \simeq 0.15\ \text{Å},\ E \approx 237.2\ \text{eV},\ J = 0.25\%,\ T = 250.2\ \text{K}.$$

The result is $\Gamma_{\text{Pd}} \approx 10^{-45}$, $P_{\text{int}} \approx 10^{-48}$.

Other values of T, Γ, and P are reported in Tables 1 and 2.

3. Conclusions

The present work has shown that microcracks and deuterium loading in the lattice at room temperature have a significant influence on the probability of fusion.

In fact, calculating the probability of interaction within a microcrack, an increase of at least 2–3 orders of magnitude are found compared to the probability of fusion on the surface. Further, with the theoretical analysis developed it is possible to obtain relatively high values for the probability of fusion for D_2 loaded impure metals at room temperature.

On the other hand, results very close to the experimental data have already been obtained without imposing the D_2 loading (e.g. for $J \approx 0.75\%$, $E \approx 250$ eV, $T = 300$ K, $\Gamma = 10^{-21}$, and $P \approx 10^{-25}$) [5]. Judging by the comparison between the two theoretical calculations, it would seem that the experimental procedure *reduces* the rate of fusion rather than enhances it. To verify the influence of the concentration of impurities on the process from another point of view, the trend of the potential within the pure lattice ($J \approx 0.25$) was evaluated and a very high curve obtained. Therefore, crossing the barrier would require a total energy greater than the potential, as shown in Fig. 1 for palladium. If the potential barrier is evaluated for the same metal with a higher level of impurity ($J \approx 0.75\%$), under the same thermodynamic conditions of the system, it is seen that the probability of fusion may be greater than that observed for pure metals, with a total energy lower than the potential so that the tunneling effect is amplified.

References

[1] F. Frisone, Can variations in temperature influence deuteron interaction within crystalline lattices? *Il Nuovo Cimento D* **20** (10) (1998) 1567–1580.
[2] G. Chambers, Evidence for MeV particle emission from Ti charged with low-energy deuterium ions, NRL Memorandum Report 6927, 18 Dec. 1991, Naval Research Laboratory, Washington, D.C. 20375–5321.
[3] C.J. Horowitz, Cold fusion in metallic hydrogen and normal metals, *Phys. Rev. C* **40** (4) (1989) 1555–1558.
[4] J. Price Hirt and J. Lothe, Theory of dislocation, *Z. Phys.* (1960) 116–129.
[5] F. Frisone, Deuteron interaction within a microcrack in a lattice at room temperature, *Fusion Technol.* **39** (2001) 260–265.

J. Condensed Matter Nucl. Sci. 1 (2007) 47–61

Research Article

Very Sizeable Increase of Gravitation at Picometer Distance: A Novel Working Hypothesis to Explain Anomalous Heat Effects and Apparent Transmutations in Certain Metal/Hydrogen Systems*

J. Dufour†

CNAM—Laboratoire des Sciences Nucléaires, 2 rue Conté, 75003 Paris, France

Abstract

Since more than 15 years, unexplained heat effects have been reported in systems involving hydrogen isotopes (hydrogen and deuterium) and certain metals like palladium. The most studied system (palladium/deuterium) has given birth to the "Cold Fusion" concept: a special kind of DD fusion reaction, only occurring in a metallic lattice, which yields heat and helium-4 as the main reaction product. Other systems have also been studied (nickel hydrogen and caesium/deuterium for instance), showing shifts in isotopic ratio of the products of reaction and leading to the more generalized concept of Low Energy Nuclear Reaction (LENR). A novel conjecture (the pico-gravity conjecture) is presented here, that may explain all the anomalies observed in this so-called "Cold Fusion" field. According to this conjecture, the main part of the energy produced in Low Energy Nuclear Reaction could be the result of a very special kind of chemical reactions (pico-chemical reactions), induced by a considerable increase of gravity at pico-meter distances (pico-gravity). True nuclear signatures (α-particles emission for instance) could also occur according to the pico-gravity conjecture. But they should be many orders of magnitude lower than would be expected from the energy produced (which is observed experimentally). This conjecture will be tested by analysing the products of the reaction of hydrogen isotopes with selected metals.

Keywords: Cold fusion, Gravity, Isotopic shift, LENR, Low Energy Nuclear Reactions

1. Introduction

For more than 15 years since 1989, claims have been made of nuclear reactions occurring in metals (palladium for instance) at room temperature in the presence of hydrogen isotopes. During the course of electrolysis of D_2O with a palladium cathode, Fleischmann and Pons [1] observed an exothermal reaction, which they interpreted as being a special kind of deuterium nuclear fusion reaction. Claims have also been made of transmutations of chemical species, inducing

*This paper was presented in ASTI, at the 7th International Workshop on anomalies in Hydrogen/deuterium loaded metals. Following a review process, a new improved version is presented here (March 2007).
†E-mail: dufourj@cnam.fr; Tel.: +33-1-40272915

isotopic composition variations. Recently, very surprising results (transmutation of cesium into praseodymium and strontium into molybdenum) have been obtained by passing a flux of deuterium through a multi-layer composite of palladium and calcium oxide [2].

Various working hypothesis have been presented to explain the occurrence of nuclear reactions in solids at energies in the order of eV [3,4]. These hypotheses address the two main problems in the field and explain by novel quantum mechanical effects in condensed matter, the overcoming of the Coulomb barrier at room temperature and the absence of the expected characteristic radiations accompanying nuclear reactions. These hypothesis are generally rejected by mainstream scientists. In that perspective, the DOE report of 1 December 2004 [4], proposes that dedicated experiments should be founded to check two types of observations: one is the anomalous character of the heat production with deuterium, the other is the particles reportedly emitted from deuterated foils, using state of the art apparatus and methods. This is an indication that the DOE report acknowledges that something unusual might occur in certain metal/hydrogen systems.

In this DOE report, observation of apparent transmutations without radiation emission [2,5] was not taken into account. Although this might be seen as a strong proof of the occurrence of nuclear reactions in condensed matter, it will be seen that these results can indeed be rationalized by the novel working hypothesis presented below.

2. The Novel Working Hypothesis

It is commonly accepted that the electromagnetic, the weak nuclear and the strong nuclear forces, have the same intensity at the quark scale (Grand unification). It is suspected that the intensity of gravity should increase when the distance decreases and that the four interactions should have the same intensity at a sufficiently small distance (Superunification). Since 1926 and the publication of the article of Kaluza [6], who proposed a model for gravitation variations with distance, the increase of gravitation has been confined to the Plank distance, but with no experimental proof. With this very restrictive concept, gravitation should increase by a factor of some 10^{40} within a distance of 10^{-33} cm (the Plank distance), which is very questionable. The attitude towards gravitation intensity variations with distance has changed during the last 20 years [7] and a great number of theoretical models embedded in string theory and with very surprising and intellectually challenging concepts await experimental results to choose those that are backed by reality. A sizeable experimental effort is carried out at tens of μm distances [8] and so far no variations have been observed down to 50 μm. This is the upper limit for experimentally allowed gravitation variations, from the known macroscopic value (6.673×10^{-11} m^3/kg s^2), towards the ultimate one expected at Plank distance (some 7×10^{29} m^3/kg s^2). Direct measurement of the Newton constant at much smaller distances seems impossible.

It is then hypothesized that the intensity of gravitation very strongly increases at distances of the order of the inner atomic distances (0 to some 100 pm). This increase is supposed to attain such a level, that the gravitational intensity attraction between a proton (or a deuteron) and a nucleus A becomes of the same order of magnitude as their Coulomb repulsion. A simplified model of the interaction between the nucleus A and the proton (deuteron) embedded in the electronic layers of A is presented. This model is purely phenomenological, no attempt being made to modelize additional dimensions of space/time. A strong increase of the gravitational constant G is indeed considered, in the ordinary four-dimensional space/time.

It will be shown that this model predicts the possibility of bound states between the proton (deuteron) and A, with binding energies of a few hundred eV. This can explain the bulk of the anomalous enthalpy of reaction observed in certain metal/hydrogen systems. This model can also explain some very faint nuclear reactions, producing only very weak typical nuclear signatures and contributing only marginally to the enthalpy of reaction.

3. The Model

The model presented below, uses the same line of reasoning as the elementary calculation of the Bohr radius and the ionisation energy of the hydrogen atom, which is described now.

3.1. Simplified Model of the Hydrogen Atom

To calculate the radius and ionisation energy of a hydrogen atom, the following simple calculation is often used: with

$$Q^2 = \frac{e^2}{4\pi\varepsilon_0},$$

m_e, v_e the electron mass and velocity and r the distance proton/electron, the potential energy of the electron is

$$E_\mathrm{P} = -\frac{Q^2}{r}$$

and its kinetic energy is $E_\mathrm{C} = (1/2)\, m_\mathrm{e} v_\mathrm{e}^2$. A bound state of the electron has a radius r that minimizes its total energy $E = E_\mathrm{P} + E_\mathrm{C}$. Taking into account Heisenberg uncertainty on momentum: $m_\mathrm{e} v_\mathrm{e} r = n\hbar$ with $n \geq 1$ (n being an integer), the total energy of the electron is

$$E = -Q^2 \frac{1}{r} + \frac{n^2\hbar^2}{2m_\mathrm{e}} \frac{1}{r^2}. \quad (1)$$

Thus,

$$\frac{\partial E}{\partial r} = \frac{1}{r^2}\left[Q^2 - \frac{n^2\hbar^2}{m_\mathrm{e}} \frac{1}{r}\right],$$

yielding the electron bound states:

$$r_n = n^2 \frac{\hbar^2}{Q^2 m_\mathrm{e}} = n^2 a,$$

with

$$a = 52.92\,\mathrm{pm}\ \text{(Bohr radius)}$$

and

$$E_n = -\frac{1}{n^2} \frac{Q^4 m_\mathrm{e}}{\hbar^2} = -\frac{1}{n^2} E_\mathrm{I},$$

with $E_\mathrm{I} = 13.6\,\mathrm{eV}$ (hydrogen ionisation energy).

Simplified model of bound states of a hydrogen nucleus surrounding an atom A, embedded in its electronic system and submitted to an hypothetical strong gravitational potential:

The above approach is used in Fig. 1.

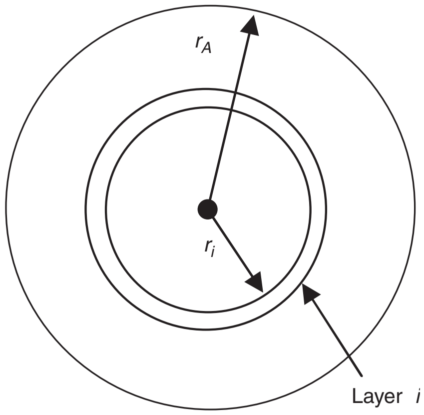

Figure 1. Simplified model of bound states of a hydrogen nucleus surrounding an atom A.

The electronic system of an atom A, having a mass number A, an atomic number Z and a radius r_A, is represented by a series of equidistant two-dimensional layers of electric charges, each layer having a charge equal to e, the electric charge of an electron. There are thus Z layers surrounding the nucleus of A, the innermost radius of layer i being:

$$r_i = \frac{r_A}{Z} i \quad \text{with} \quad 0 < i \leq Z - 1.$$

A hydrogen nucleus approaching atom A from outside will be submitted to two potentials:

(1) The repulsive Coulomb potential of the nucleus of A, which will be less an less screened by the electron layers as it moves towards the nucleus of A: $E_P^E = (Z - i)\, Q^2 \frac{1}{r_i}$.
(2) The attractive gravitational potential of A: $E_P^G = -G' A m_p m_H 1/r_i$, G' being the increased Newtonian gravitation constant, m_p the mass of the proton (the mass difference between the proton and the neutron and the mass corresponding to the binding energy of the nucleus being neglected) and m_H the mass of the hydrogen isotope under study. The total energy of the hydrogen nucleus is thus

$$E = \left[(Z - i)\, Q^2 - G' A m_p m_H\right] \frac{1}{r} + \frac{n^2 \hbar^2}{2 m_H} \frac{1}{r^2} = -k\,(Z - i)\, Q^2 \frac{1}{r} + \frac{n^2 \hbar^2}{2 m_H} \frac{1}{r^2} \tag{2}$$

with

$$k = \frac{G' A m_p m_H}{(Z - i)\, Q^2} - 1 \tag{3}$$

using for (2) the same method as for (1), yields the hypothetical bounds states of the hydrogen nucleus, embedded in the electronic system of A, submitted to a combined Coulomb and gravitational potential of intensity G' and round its nucleus:

$$r_n = \frac{n^2 \hbar^2}{k\,(Z - i)\, Q^2 m_H} = n^2 a \frac{1}{k\,(Z - i)} \frac{m_e}{m_H}, \tag{4}$$

$$E_n = -\frac{1}{2}\frac{k^2\,(Z-i)^2\,Q^4 m_\mathrm{H}}{n^2\hbar^2} = -\frac{1}{n^2}E_\mathrm{I}k^2\,(Z-i)^2\,\frac{m_\mathrm{H}}{m_\mathrm{e}}. \tag{5}$$

Remark: Through all this article and to distinguish the hydrogen isotopes under study, the following notations will be used for their nuclei.

Generic denomination: H for both isotopes

(1) Hydrogen (one proton) p.
(2) Deuterium (one proton, one neutron) d.

4. Discussion

For solutions to exist, k (3), must be positive. The minimum required value of the increased Newtonian gravitation constant is thus

$$G' = \frac{(Z-i)Q^2}{A m_\mathrm{p} m_\mathrm{H}},$$

obviously corresponding to a very sizeable increase of the intensity of gravitation. It can also be seen that the exact required minimum value of G' depends upon the system under study. It will be much higher for the hydrogen/hydrogen system ($A = 1, m_\mathrm{H} = m_\mathrm{p}$), than for the $^{206}_{82}$Pb/deuterium system for instance ($A = 206, m_\mathrm{H} = 2m_\mathrm{p}$).

The simpler system (in term of number of protons and neutrons involved) that has been observed experimentally to yield reactions will thus fix the value of G'. This value can then be used to study more complicated reactions. The deuterium/deuterium case seems to be a good candidate to determine G' For the sake of simplicity, we shall call “pico-gravity” the strongly enhanced gravity at picometer distances with an apparent newtonnian constant G'.

4.1. Interaction of Two Deuterium Nuclei

Although, the simple model presented is even more oversimplified in that case (the centre of mass of the system is in between the two deuterium nuclei), it is used to give an order of magnitude of G'

Equation (4) gives

$$r_1 = a\frac{1}{k_\mathrm{d,d}}\frac{m_\mathrm{e}}{m_\mathrm{H}} \approx a\frac{1}{k_\mathrm{d,d}}\frac{m_\mathrm{e}}{2m_\mathrm{p}} = 2.7\times10^{-4}\frac{a}{k_\mathrm{d,d}}.$$

Thus,

$$k_\mathrm{d,d} = 2.7\times10^{-4}\frac{a}{r_1}.$$

It is known that in a deuterium molecule, the distance between the two deuterium nuclei is some 74 pm. With this distance, nuclear fusion reactions between the two nuclei are extremely rare. On the contrary, in a mesic deuterium molecular ion, this distance is some 200 times smaller (0.4 pm), yielding a reaction time of a few μs. It has been observed that deuterium trapped in a palladium lattice yields very small amounts of tritium, neutron and helium 4. The amounts of helium 4 observed are much larger than would be expected from a classical “hot fusion reaction” and the helium 4 looks like the major product of the “cold fusion reaction” observed. Another plausible explanation for the apparition of sizeable amounts of helium 4 and heat in a lattice where a “cold fusion reaction” occurs will be discussed later. For the time being, it is hypothesized that a classical "hot fusion reaction" can be catalysed by pico-gravity, through the formation of a compound with a size smaller than 74 pm, but much bigger than 0.4 pm, yielding a very small but measurable rate of "hot fusion" reactions with associated heat and classical products pattern. The determination of the exact value would require more experiments to determine the exact rate of the reaction and thus the exact value of r_1. In first approximation, r_1 is set at 20 pm, finally yielding

$$k_{\mathrm{d,d}} = 7.15 \times 10^{-4}$$

and

$$G' = \left(1 + k_{\mathrm{d,d}}\right) \frac{Q^2}{4m_{\mathrm{p}}^2} \approx 2.06 \times 10^{25}\ \mathrm{m}^3\ \mathrm{kg}^{-1}\ \mathrm{s}^{-2}, \tag{6}$$

which is a 3×10^{35}-fold increase compared to the measured macroscopic value ($6.67 \times 10^{-11}\mathrm{m}^3\ \mathrm{kg}^{-1}\ \mathrm{s}^{-2}$). It will be shown below that this increase can well have been hidden in all presently known systems, because of its very weak effects in such systems.

Using this value of G' for the pico-gravity constant, the interactions of hydrogen isotopes with atoms with mass number higher than two are now examined.

5. Interaction of Hydrogen Isotopes with Atoms with Atomic Number $Z \geq 2$ and Mass Number A

To explicit Eqs. (4) and (5), the value for G' is taken equal to the value calculated from the interaction d,d and given by (6):

$$G' = \left(1 + k_{\mathrm{d,d}}\right) \frac{Q^2}{4m_{\mathrm{p}}^2}.$$

Thus,

$$k_{\mathrm{A,H}} = \frac{G' A m_{\mathrm{P}} m_{\mathrm{H}}}{(Z-i)\, Q^2} - 1 = \frac{m_{\mathrm{H}}}{4m_{\mathrm{p}}} \frac{A}{(Z-i)} \left(1 + k_{\mathrm{d,d}}\right) - 1.$$

Thus,

$$r_n = n^2 a \frac{1}{k_{\mathrm{A,H}}\,(Z-i)} \frac{m_{\mathrm{e}}}{m_{\mathrm{H}}} = n^2 a \frac{m_{\mathrm{e}}}{m_{\mathrm{H}}} \left[\frac{1}{\frac{m_{\mathrm{H}}}{4m_{\mathrm{p}}} A \left(1 + k_{\mathrm{d,d}}\right) - (Z-i)} \right] = n^2 a \frac{m_{\mathrm{e}}}{m_{\mathrm{H}}} K\,(i)\,, \tag{7a}$$

with

$$K\,(i) = \frac{1}{\frac{m_{\mathrm{H}}}{4m_{\mathrm{p}}} A \left(1 + k_{\mathrm{d,d}}\right) - (Z-i)} \tag{7b}$$

and

$$E_n = -\frac{1}{n^2} E_{\mathrm{I}} k_{\mathrm{A,H}}^2\,(Z-i)^2 \frac{m_{\mathrm{H}}}{m_{\mathrm{e}}} = -\frac{1}{n^2} E_{\mathrm{I}} \frac{m_{\mathrm{H}}}{m_{\mathrm{e}}} L\,(i)\,, \tag{8a}$$

with

$$L\,(i) = \frac{m_{\mathrm{H}}^2}{16 m_{\mathrm{p}}^2} A^2 \left(1 + k_{\mathrm{d,d}}\right)^2 - \frac{m_{\mathrm{H}}}{2 m_{\mathrm{p}}} A \left(1 + k_{\mathrm{d,d}}\right) (Z - i) + (Z - i)^2. \tag{8b}$$

Equations (7a) and (8a), describe the possible bound states of H in the combined Coulomb + gravitational field of A. H entering the electronic layers of A from the outside, n should decrease as H approaches the nucleus of A. For the model to be coherent, n is determined as a function of i by writing:

$$r_i = \frac{r_{\mathrm{A}}}{Z} i = r_n = n^2 a \frac{m_{\mathrm{e}}}{m_{\mathrm{H}}} K\,(i)\,.$$

Thus,

$$n = \sqrt{\frac{r_{\mathrm{A}}}{a} \frac{m_{\mathrm{H}}}{m_{\mathrm{e}}} \frac{i}{Z K\,(i)}}. \tag{9}$$

In the regions of interest, n is high; r_n and E_n are thus calculated by taking the integer value of n given by (9). The discrepancy between r_i and r_n is small.

Equations (7a), (7b), (8a), (8b) and (9) shall be used to study the interaction of a proton (p) and a deuteron (d) with various atoms A and their isotopes (r_{A} is taken equal to the covalent radius of A). The values of $K(i)$ and $L(i)$ given by (7b) and (8b) are calculated for both hydrogen isotopes as will be seen below.

6. Interaction of a Proton (p) with an Atom A

In this case,

$$K\,(i) = \frac{1}{\frac{1}{4} A \left(1 + k_{\mathrm{d,d}}\right) - (Z - i)}. \tag{10a}$$

The progression of p towards the nucleus of A is limited to the layers with

$$i > Z - \frac{A}{4}\left(1 + k_{\mathrm{d,d}}\right) \approx Z - \frac{A}{4} \ (k_{\mathrm{d,d}} \text{ is small compared to 1})$$

and the minimum value for i is

$$i_{\min} = Z - \frac{A}{4} + 1,$$

for which $K\,(i_{\min}) = 1$. In other word, when the screening by electrons becomes insufficient ($i < Z - A/4$), the Coulomb repulsion gets higher than the pico-gravity attraction and the proton is repelled. An equilibrium can nevertheless be attained, the proton oscillating between the layers $i_{\min}$ and $i_{\min} + 1$.

Hence,

$$r_{\min} = \frac{r_{\mathrm{A}}}{a} \frac{m_{\mathrm{H}}}{m_{\mathrm{e}}} a \frac{m_{\mathrm{e}}}{m_{\mathrm{H}}} \frac{i_{\min}}{Z K\,(i_{\min})} = r_{\mathrm{A}} \frac{Z - \frac{A}{4} + 1}{Z}. \tag{10b}$$

The proton p can thus never come to the close vicinity of the nucleus of A. Compounds formed will contain proton(s) embedded in the outer electronic layers of A.

$$L\left(i\right)=\frac{m_{\mathrm{H}}^{2}}{16m_{\mathrm{p}}^{2}}A^{2}\left(1+k_{\mathrm{d,d}}\right)^{2}-\frac{m_{\mathrm{H}}}{2m_{\mathrm{p}}}A\left(1+k_{\mathrm{d,d}}\right)\left(Z-i\right)+\left(Z-i\right)^{2}$$
$$=\frac{A^{2}}{16}\left(1+k_{\mathrm{d,d}}\right)^{2}-\frac{A}{2}\left(1+k_{\mathrm{d,d}}\right)\left(Z-i\right)+\left(Z-i\right)^{2}\approx\left[\frac{A}{4}-\left(Z-i\right)\right]^{2}. \tag{11}$$

Thus, the energy of the proton is always negative, and at the layer $i=i_{\min}\approx Z-\frac{A}{4}+1$, $L\left(i_{\min}\right)=1$. The value of the energy at $i_{\min}$ is then

$$E_{i_{\min}}=-\frac{a}{r_{\mathrm{A}}}E_{\mathrm{I}}\frac{2K\left(i_{\min}\right)L\left(i_{\min}\right)}{i_{\min}}=-\frac{a}{r_{\mathrm{A}}}E_{\mathrm{I}}\frac{2}{Z-\frac{A}{4}+1}.$$

Examples of the variation of the proton energy with its distance to the nucleus of various atoms A are given below. Calculations are made using Eqs. (7a), (8a), (9), (10a) and (11).

7. Interaction of a Deuteron (d) with an Atom A

In this case,

$$K\left(i\right)=\frac{1}{\frac{1}{2}A\left(1+k_{\mathrm{d,d}}\right)-\left(Z-i\right)} \tag{12}$$

is always positive (in stable isotopes $A\geq 2Z$). The deuteron could come to contact with the nucleus of A (for $n=1$, values of r_n are of the size of a nucleus). This might happen in rare cases, and could result in a nuclear reaction (fission, α emission, …). But in most cases it is likely that its progression is limited by Pauli exclusion principle, the electrons between the deuteron(s) and the nucleus of A having less and less energetic levels available as the deuteron d progresses towards A, in a way comparable of what is considered in the calculation of Chandrasekhar's limit for white dwarf stars. This is confirmed by the very low intensity of typical nuclear radiations experimentally observed. It is assumed that Pauli exclusion principle sets the minimum distance between the deuteron(s) and the nucleus of A. To visualize, on the graphs presented below, the possible effect of the Pauli exclusion principle, a repulsive Lennard–Jones type of potential (A/r^{12}) has been added to the combined Coulomb/gravitational potential. This potential has been set empirically, hypothesizing that the 2 s electrons are involved, which gives an order of magnitude of the distance at which the minimum total energy of the system occurs. The complex atom formed could have atomic characteristics close to but different from the product of a nuclear reaction between A and d [8]. This point will be discussed in details below.

$$L\left(i\right)=\frac{A^{2}}{4}\left(1+k_{\mathrm{d,d}}\right)^{2}-A\left(1+k_{\mathrm{d,d}}\right)\left(Z-i\right)+\left(Z-i\right)^{2}\approx\left[\frac{A}{2}-\left(Z-i\right)\right]^{2} \tag{13}$$

is always positive. The total energy of the deuteron is thus always negative.

Examples of the variation of the deuteron energy with its distance to the nucleus of various atoms A are given below. Calculations are made using Eqs. (7a), (8a), (9), (12) and (13).

8. General Comments on the Proposed Model

Due to the simplified character of the model presented, only a rough order of magnitude can be expected when using it to describe this novel type of chemical reactions between a hydrogen isotope and an atom A. Anyhow, it will be seen that there is a general concordance between its predictions and what has been observed in the so-called LENR field (Low Energy Nuclear Reaction).

A second point must be stressed. An infinite range of the strong gravity has been considered, resulting in a sizeable attractive potential at the limit of the atom A (orders of hundred eV). Such a potential should already have been seen. In fact the range of strong gravity should be limited, probably at values lower than 100 pm, that is lower than typical atom size. This point will be discussed below in details. In the graphs that are presented in the following paragraph, this limitation has not been taken into account. Some of the reactions described in these graphs could not occur, if the range of pico-gravity is too small.

A third point is worth being noted: the proton and the deuteron behave differently. The mass of the latter is sufficient to insure an attractive combined Coulomb gravitational potential, even at very short distance from the nucleus of A. An equilibrium position can be found between this attractive combined potential and the repulsive potential created by the Pauli exclusion principle.

On the contrary, the progression of the proton towards the nucleus of A is limited to a minimum distance [Eq. (10b)]. Anyhow, an equilibrium could be reached, the proton oscillating round its minimum distance from the nucleus of A given by Eq. (10b), but it is likely that reactions with hydrogen should be less frequent and with a lower rate than those observed with deuterium. In other words, the pico-gravity conjecture explains heat production with deuterium. In certain favourable cases (nickel and compact atoms for instance) hydrogen could also react. This will be exemplified below.

9. Examples of Bound States of Hydrogen Isotopes with Selected Atoms A

The case of four atoms A will be examined: nickel, palladium, caesium and strontium.

9.1. Case of Nickel

The calculation has been made for the most abundant nickel isotope ($^{58}_{28}$Ni, 68%). Results are displayed in Fig. 2, giving the total energy of the hydrogen isotope as a function of the distance to the nucleus of Ni.

For deuterium, a bound state could occur with binding energy of some 200 eV. For hydrogen, as explicited above, the proton could oscillate at a distance $r_{\min}$ of some 55 pm from the nickel nucleus with a binding energy round 350 eV.

The type of radiation expected is a copious emission of very low energy X-rays, more likely to be detected as heat in the calorimeter. Heat generation has indeed been observed in the system Nickel/Hydrogen [10].

The rate of reaction should vary with the various isotopes of nickel (influence of A), giving rise to an apparent isotopic change in the remaining unreacted nickel.

As regards the products formed, they could mimic (depending upon the analytical method used) atoms A$'$ resulting from the addition of proton(s) or deuteron(s) to the nucleus of A. This point will be discussed in detail below in the case of caesium and strontium.

9.2. Case of Palladium

The calculation has been made for the most abundant palladium isotope ($^{106}_{46}$Pd, 28%). Results are displayed in Fig. 3, giving the total energy of the hydrogen isotope as a function of the distance to the nucleus of Pd.

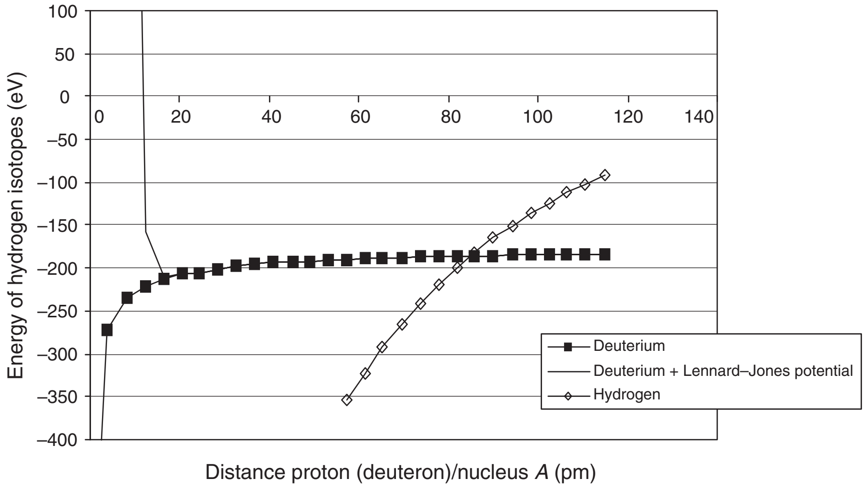

Figure 2. Bound states of hydrogen isotopes with Nickel (58).

For deuterium, a bound state could occur with binding energy of some 800 eV. For hydrogen, the binding energy should be less, round 650 eV corresponding (as for nickel) to the layer $i_{\min}$. Same considerations as for nickel, apply for the other characteristics of this reaction.

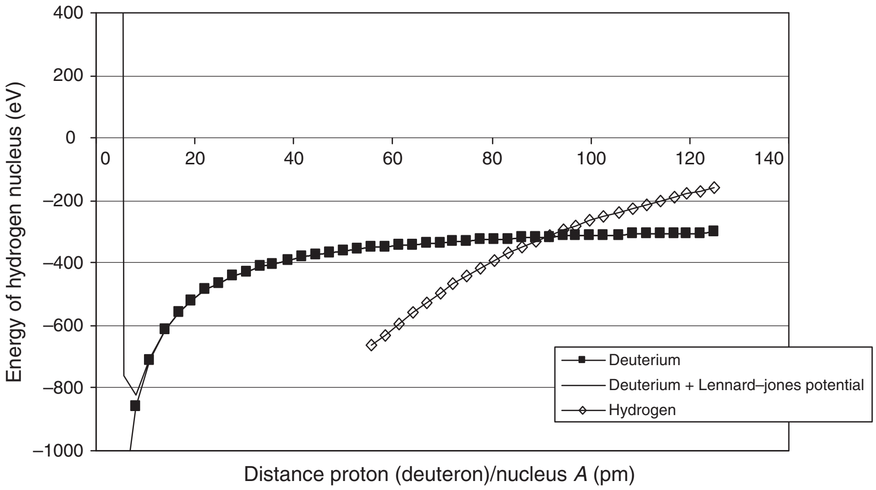

Figure 3. Bound states of hydrogen isotopes with palladium (106).

9.3. Case of Caesium

The calculation has been made for the sole stable caesium isotope ($^{133}_{55}$Cs, 100%). Results are displayed in Fig. 4, giving the total energy of the hydrogen isotope as a function of the distance to the nucleus of Cs.

For deuterium, a bound state could occur with binding energy of some 1200 eV. For hydrogen, the binding energy should be very low: 50–100 eV and decreases when the distance proton nucleus decreases.

In that case, the energy for $i_{\min}$ is very low and it is very unlikely that the proton could oscillate round $r_{\min}$ as for Nickel and hydrogen. Caesium could even not react with hydrogen, the distance at which the combined Coulomb gravitational potential becomes repulsive being some 70 pm, which might be to close to the maximum range of pico-gravity.

The case of caesium has been the object of extensive experimental studies [2,5]. By permeating deuterium through a complex layered structure of palladium and calcium oxide, containing minute amounts of caesium, the apparent following nuclear reaction has been observed (with various experimental techniques):

$$^{133}_{55}\mathrm{Cs} + 4^{2}_{1}\mathrm{H} \rightarrow {}^{141}_{59}\,\mathrm{Pr}, \;\; Q = 50.5\,\mathrm{MeV}. \tag{14}$$

The Q-value was calculated from the mass defect of Eq. (14).

Should reaction (14) occur, copious fast neutrons would be generated (they where not observed). It is unlikely that the majority of the energy could be passed to fission fragments (because of the Coulomb barrier) or to gamma rays (because of the slow electro-magnetic transition).

Following analytical techniques were used to characterize the apparently formed praseodymium:

(1) In situ X-ray Photoelectron Spectroscopy (XPS) for most of the experiments.
(2) X-ray Absorption Near Edge Structure (XANES) for some experiments.
(3) TOF SIMS for a few experiments.

Results of in situ *XPS*: they show the clear disappearance of the caesium LM lines and the concomitant appearance of the praseodymium LM lines.

Results of XANES: they confirm the results of in situ XPS.

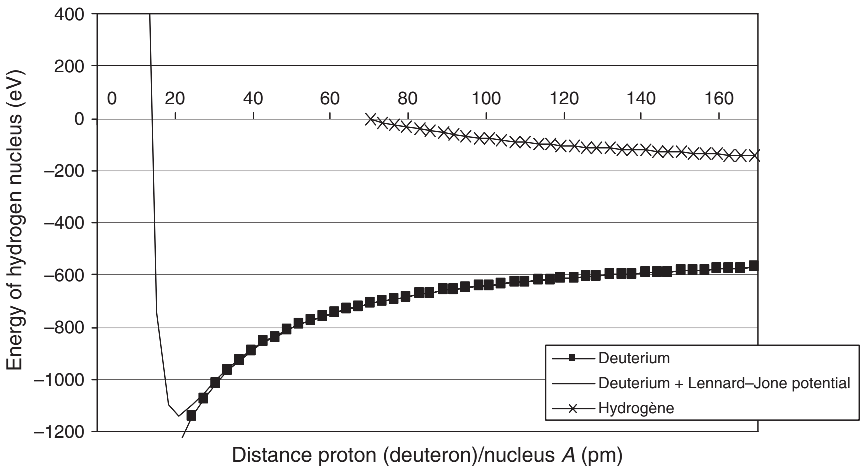

Figure 4. Bound states of hydrogen isotopes with caesium (133).

Results of TOF SIMS: they clearly show the appearance of an atom with mass 140.90 very close to the mass of praseodymium (140.908). No standard deviation of this result is given: TOF SIMS has a very high resolution, but it cannot be excluded that the absolute value found is not exactly 140.90: it could be closed to, but different from this value. This point will be discussed below.

9.4. Case of Strontium

The calculation has been made for the most abundant strontium isotope ($^{88}_{38}$Sr, 82.6%). Results are displayed in Fig. 5, giving the total energy of the hydrogen isotope as a function of the distance to the nucleus of Sr.

For deuterium, a bound state could occur with binding energy of some 800 eV. For hydrogen, the binding energy should be in the order of 50–100 eV. As for caesium, the existence of a minimum of the total energy for the proton, will depend upon the exact range of the increased gravity, which, as stated before, has not been taken into account in Fig. 5. As for caesium, strontium could even not react with hydrogen.

As for caesium, the case of strontium has been the object of extensive experimental studies [2,5]. By permeating deuterium through a complex layered structure of palladium and calcium oxide, containing minute amounts of strontium, the apparent following nuclear reaction has been observed (with various experimental techniques):

$$^{88}_{38}\mathrm{Sr} + 4^{2}_{1}\mathrm{H} \rightarrow {}^{96}_{42}\mathrm{Mo}, \quad Q = 53.5\,\mathrm{MeV}. \tag{15}$$

The Q-value was calculated from the mass defect of Eq. (15).

Following analytical techniques were used to characterize the apparently formed molybdenum:

(1) In situ XPS for most of the experiments.
(2) Secondary Ion Mass Spectroscopy (SIMS) for many experiments.

Results of in situ XPS: they show the clear disappearance of the strontium lines and the concomitant appearance of the molybdenum lines.

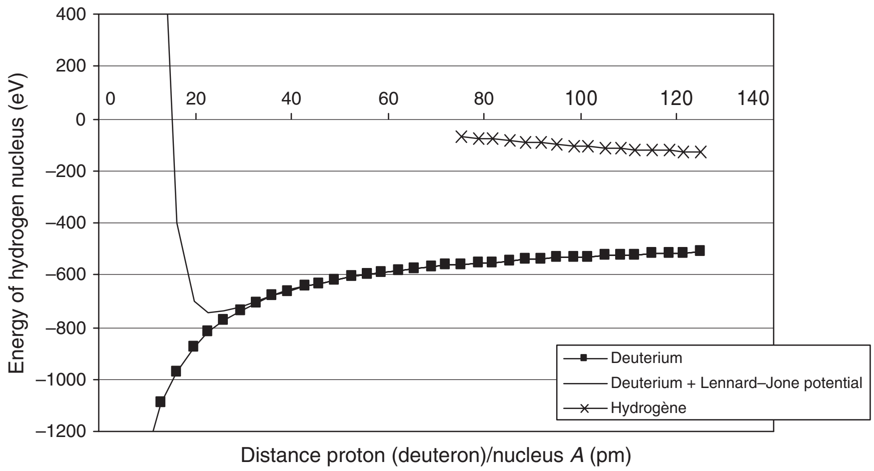

Figure 5. Bound states of hydrogen isotopes with strontium (88).

Results of SIMS: the product of strontium transformation has an isotopic composition very different from that of natural molybdenum. The major "molybdenum" peak is $^{96}_{42}Mo$. The major isotope of strontium is $^{88}_{38}Sr$. It is thus tempting to attribute the formation of Mo to reaction (15) and the similar ones for the other strontium isotopes

9.5. General Comments for the Case of Caesium and Strontium

All experimental observations described above, together with the absence of reaction with hydrogen, have been presented as strong evidence for nuclear reactions (14) and (15) to occur in solids.

The model presented here gives a simple and semi-quantitative description of another possible mechanism:

Four deuterons bind to the nucleus as described above (the proposed model is too simple to confirm or refute the assumption made that four deuterons could bind) and form a complex compound that can be written: $\left[^{88}_{38}Sr, 4^{2}_{1}H\right]or\left[^{133}_{55}Cs, 4^{2}_{1}H\right]$.

As these deuterons are close to the nucleus of strontium or caesium, the external electronic layers of the compound formed, see in fact a molybdenum or praseodymium nucleus and this is what XPS or XANES describe. The isotopic variation observed for the case of strontium is also a straightforward consequence of the model.

Remains the case of the mass of the "praseodymium" formed: the mass of $^{141}_{59}$ Pr is 140.9076.

The mass of $\left[^{133}_{55}Cs, 4^{2}_{1}H\right]$would be very close to 140.9614, a 380 ppm difference with the mass of Pr, that can be distinguished by TOF SIMS. What is questionable is the absolute calibration of the apparatus and this point would be worth being studied in details. A measure of the standard deviation is a must, together with an absolute calibration of the system.

10. Pico-gravity Conjecture and Other Observations in the Field of So-called Cold Fusion

10.1. Helium-4 Production

It has been observed experimentally (as mentioned in Section 4.1) that excess heat frequently occurs with the production of helium 4 in quantities many orders of magnitude higher than would be expected from a "hot fusion" reaction. This helium production has been ascribed to a special kind of dd fusion reaction where helium 4 is the main product. Another plausible scenario to explain this (apparent) helium 4 production is the following:

(1) Case of deuterium and palladium: the expected energy per pico-chemistry reaction in that case, is some 800 eV. It is likely that any helium 4 in the surroundings of the reacting palladium atom would get sufficient energy to be expelled from the lattice and measured as "reaction product". In these circumstances, any correlation between the energy produced and the helium measured would only reflect the initial helium 4 content of the lattice. It is interesting to note that there is a great dispersion in the measured values of the energy per atom helium 4 produced in the case of palladium (the most studied system).
(2) Case of hydrogen: as mentioned above, the reaction with hydrogen according to the pico-gravity conjecture is less probable, with a lower rate than with deuterium and likely to be limited to compact atoms like nickel. Data are lacking on a possible (apparent) production of helium 4 in that case.

10.2. "True" nuclear reactions

Nuclear signatures at very low level, as alphas or fast charged particles, have been observed in certain experiments. These can be accounted for by the pico-gravity conjecture. Consider the case of deuterium and palladium. As mentioned above, in very rare occasions the deuteron could reach the nucleus of the atom A and react with it. As an example, the following reaction could be observed:

$$^{105}_{46}\mathrm{Pd} + ^{2}_{1}\mathrm{H} = ^{103}_{45}\mathrm{Rh} + +^{4}_{2}\mathrm{He}, \quad Q = 10.8\ \mathrm{MeV}$$

yielding fast alphas and lower mass isotopes (transmutation in lighter isotopes).

11. Range of the Increased Pico-gravity and Possible Effects on Known Systems

In the modern concept of gravitation increase, additional space dimensions open at a given range.

Modelling such concept is far beyond the scope of this note. One requirement is that this opening does not conflict with known physic and chemistry. So the range of these new dimensions should be well within atom size. A range between some 50 and 100 pm seems realistic. Known chemistry would not have seen them. Inside the atom and due to the very small mass of an electron, the electronic layers would not be altered in a measurable way. There remains the case of the Lamb shift which is related to the mass of the electron. The overall mathematical treatment of the effect of the pico-gravity conjecture combined with quantum electrodynamics is probably extremely complex. Should this problem find a solution, an explanation could be found for the discrepancies observed between the predicted value and the most recent experimental measurements of this Lamb shift [11].

The finite range of these new dimensions also requires gravity to be carried along these dimensions through a massive graviton. An estimation of the mass of this graviton, is given by the Yukawa relation between its range r_{G} and its mass m_{G}:

$$r_{\mathrm{G}} = \frac{\hbar}{m_{\mathrm{G}}c} \quad (\text{with } c = \text{speed of light}) . \tag{16}$$

For $r_{\mathrm{G}} = 50$ pm, Eq. (16) yields $m_{\mathrm{G}} \approx 5$ keV. The minimum detectable mass of a particle being some 250 keV, this graviton would presently be undetectable. But this mass could explain why cross sections in reactions involving its action should be energy dependant. This might be an explanation of the discrepancies observed in the cross section of a deuteron beam and a deuterated target at very low energy of the deuteron, when compared to the cross section predicted by high-energy experiments [9].

One of the main practical problem, which could be due to the limited range of this hypothetical strong gravity, would be the need for a sizeable activation energy (tens of eV), to obtain a pico-chemistry reaction. Indeed, before reaching that range, the proton (deuteron) would be submitted to the full Coulomb repulsion of the nucleus of A. Some of the reactions presented in the above graphs, may be very difficult (if not impossible) to obtain.

Finally at femtometer scale, this increased gravitation would anyhow be some 10^{-4} weaker than the strong nuclear force and acting on quarks with mass close to 1/3 the mass of protons would have an ever weaker effect: strong gravity as required by the present model would also have been unnoticed. As regards the weak nuclear force at attometer scale, things are less clear, but two of the particles involved (electron and neutrino) have a small mass, probably closed to zero for the latter.

It is obvious that a great number of questions are still to be answered. Detailed study of the formation and characteristics of compounds such as, for example $\left[^{133}_{55}\mathrm{Cs},4^{2}_{1}\mathrm{H}\right]$, should shed more light on all those questions.

12. Conclusions

The novel working hypothesis proposed could open a new field of chemistry. It is proposed to call this new field “pico-chemistry”. In pico-chemistry enthalpies of reaction are some 100 times higher than ordinary chemical reactions (oil combustion for instance).

Moreover, a better knowledge of the variations of the gravitational constant with distance could help reconcile quantum mechanics and relativity. A massive graviton, with mass round 5 keV is predicted.

References

[1] M. Fleischmann, S. Pons, Electrochemically induced nuclear fusion of deuterium, *J. Electroanal. Chem.* **261** (1989) 301.

[2] Y. Iwamura et al., Low energy nuclear transmutation in condensed matter induced by D_2 gas permeation through Pd complexes: correlation between deuterium flux and nuclear products, *Proceedings of the ICCF10* Cambridge, MA, 2003. Available at http://www.lenr-canr.org/.

[3] A. Takahashi, Mechanism of deuteron cluster fusion by EQPET model, *Proceedings of the ICCF 10,* Cambridge, MA, 2003. Available at http://www.lenr-canr.org/.

[4] DOE, Report of the review of low energy nuclear reactions December 1, 2004. Available at http://www.science.doe.gov/Sub/News_Releases.

[5] Y. Iwamura et al., Observation of surface distribution of products by X-ray fluorescence spectrometry, during D_2 gas permeation through Pd complexes, *Proceedings of the 12th International Conference on Condensed Matter Nuclear Science*, Yokohama, Japan, 2005.

[6] T. Kaluza, *Preuss. Acad. Wiss.* **K1** (1921) 966.

[7] L. Randall, Extra dimensions and warped geometries, *Science* **296** (2002) 1422.

[8] E.G. Adelberger, Available at http://xxx.lanl.gov/abs/hep-ex0202008.

[9] A. Kitamura et al., Experiments on condensed matter nuclear events in Kobe University *ICCF11 Proceedings* **218** (2004).

[10] F. Piantelli, Hydrogen loading of Ni and related phenomena, *Proceedings of SIENA 2005 Workshop*, see internet site http://www.iscmns.org/siena05/Montalbano.ppt.

[11] M. Weitz et al., Precision measurement of the hydrogen and deuterium 1s ground state Lamb shift, *Phys. Rev. Lett.* **72** (1994) 328–331.

J. Condensed Matter Nucl. Sci. 1 (2007) 62–85

Research Article

Deuteron Cluster Fusion and ASH

Akito Takahashi*

Osaka University, Yamadaoka 2-1, Suita, Osaka 565-0871, Japan

Abstract

This is a review of our studies on theoretical model of deuteron cluster fusion in condensed matter. Considering a transient condensation process of deuteron-cluster in focal points of metal–deuteride lattice, electron screening effect was theorized by the Electronic Quasi-Particle Screening Theory (EQPET) model for a transient deuteron cluster associating attracted electrons. Multi-body resonance fusion of deuterons was proposed by modeling charged-pion exchange for strong interaction in very condensed deuteron cluster to lead to select the tetrahedral resonance fusion (TRF) of 4D and octahedral resonance fusion (ORF) of 8D as possible major reaction channels in extreme case. ^{4}He is the final product of TRF and ORF. Tritium and ^{3}He was suggested as minor products from 3D multi-body fusion. Visible but very small level production of neutron by D + D (2D) fusion was also concluded. Further extension of EQPET model is given to propose a dynamic Bose-type condensation process by orthogonally coupled two D_2 molecules, which play a role of super screening of Coulomb barrier with quadruplet electronic quasi-particle to generate clean fusion product of ^{4}He.

Keywords: Ash, Bosonization, Deuteron cluster fusion, Electronic quasi-particle screening, 4D Fusion, 8D Fusion, Helium-4, Secondary reaction

1. Introduction

The possible occurrence of low energy deuteron fusion in condensed matter at room temperature, so called cold fusion, and other nuclear reactions in solid has been studied in the last 15 years since 1989 by number of people in the world, in spite of totally negative responses [1] by established scientific societies in 1989–1990. Many international conferences [2–10] have been held and numerous papers have been published in journals. Many claims of anomalous observation of excess heat, neutrons, helium, X-rays, charged particles, etc., which are asserted to evidences of "new" nuclear reactions in condensed matter, have been made. However, people have got failed to replicate the claimed results in most cases. Nevertheless, several groups have obtained physically same results for the following key observations.

(A) Generation of large amount of helium-4 (^{4}He), comparable to observed level of excess heat (1–100 W level) in PdDx systems of electrolysis-type experiments, has been confirmed by several groups [11–15,53,54]. In these

*E-mail:akito@sutv.zaq.ne.jp

experiments, neutrons and gamma-rays have not been observed with clearly countable level [16,17]. However, emission of continuous X-rays in the region less than 100 keV has sometimes been observed [18,19]. These results suggest us that some "unknown" nuclear reactions took place emitting energetic α-particles, which produced secondary continuous X-rays in slowing down with condensed matter (PdDx) and make energy deposit, comparable to excess heat, as lattice vibration. The known free particle d–d reaction, which is known to emit 2.45 MeV neutron plus 0.8 MeV ^{3}He and 3 MeV proton plus 1 MeV triton, cannot be candidate for explaining observed results.

In the text, d denotes deuteron-particle and D does deuteron with electron.

(B) Observations of anomalous amount of "foreign" elements on metal surface (cathode or permeation sample) region have been claimed by several groups [19–23]. Some new class of low-energy "nuclear transmutation" like "clean fission" without hard γ-ray radiation has been proposed by the researchers. Especially, the latest claim by Mitsubishi H. I. Group [24–27] is extraordinary; They have shown clear-cut results of generation of mass(A)-8-and-charge(Z, atomic number)-4 increased elements (^{96}Mo and ^{141}Pr form ^{88}Sr and ^{133}Cs, respectively), with large amount (10^{14} atoms per week or so), closely related to comparable reduction of test elements (Sr and Cs), by the deuterium gas permeation through multi-layered Pd/CaO/Pd film on which test elements were mounted. How is the selective occurrence of A-8-and-Z-4 increased transmutation made possible ? This is a big challenge to theoretical modeling.

Many theoreticians, and even experimentalists, have made great efforts to propose new theoretical models for "nuclear reaction in condensed matter" and attempted to consistently explain those anomalous observations. A comprehensive review paper [28] exists for the research period of 1989–1994; No theory work was enough consistent to match both of explaining anomalous results and not-violating established physics, although we may have some hopes to several models. Progress in theoretical study was rather slow in 1995–2001. However, well-cited models by researchers have been gradually converged to "coherent fusion" models. Dynamic behavior of deuterons in condensed matter, namely dynamics of solid-state-physics, may induce special conditions to make deuterons "coherent fusion," in either nm-size domain of metal–deuteride (MDx) lattice [28, 29] or more microscopic focal points in MDx lattice [30–34].

The author first proposed multi-body (three-body D + D + D) fusion model [35] as a cascade D-catalyzed reaction: D + D to ^{4}He*, ^{4}He*+ D to d + α + 23.8 MeV in very short time interval, to explain the original claim [36] on large excess heat with anomalous small level of tritium and neutron. Since that time, the author and his collaborators have elaborated [30–32] the multi-body deuteron fusion model in MDx dynamics, to meet the consistency requirements in views of established physics and to attempt to make quantitative studies on reaction rates of "cluster deuteron fusion process," which is another name of multi-body deuteron fusion in condensed matter. Especially in the latest paper [51], for ICCF9 Proceedings, the author has proposed the model of tetrahedral (TRF) and octahedral resonance fusion (ORF) in dynamic condition of PdDx ($x > 1$) lattice, considering the generation of transient "bosonization" of electrons at focal points to make super-screening of Coulomb repulsive force of d–d interaction to enhance resonantly strong interactions for 4D and 8D cluster fusion. Quantitative estimations of cluster fusion have ever been done [31,37,38,60,62]. Further elaboration done is reviewed in this work; the electronic quasi-particle expansion theory (EQPET) model was proposed by the author [48] and some numerical estimations were done by using calculations of screened potentials for dde* (e*; quasi-particle of electrons like Cooper pair and quadruplet-coupling) and dde*e* transient molecular states, to obtain very positive results to support the occurrence of deuteron cluster fusion as 4D or 3D multi-body fusion in PdDx lattice with so large reaction rate level as comparable to experimentally claimed level of excess heat and ^{4}He production. Nuclear transmutation by high-energy ^{8}Be emission of 8D cluster fusion was also proposed [51] to explain the extraordinary Mitsubishi results [24–26]. The model was further extended [60,62] to model super-screening mechanism by quasi-particle of quadruplet electrons with orthogonally coupled two D_2 molecules.

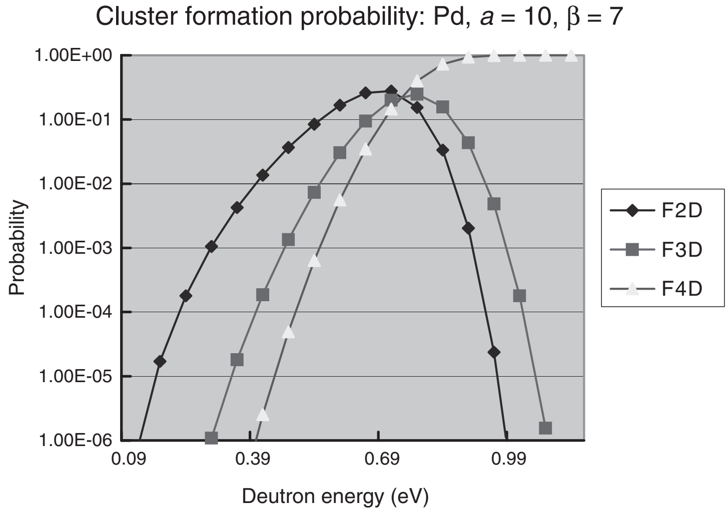

Figure 1. Cluster formation probabilities of 2D, 3D, and 4D condensation [31].

This paper first reviews the EQPET theory of deuteron cluster fusion in condensed matter, to draw a comprehensive story of the model, formulation of equations, quantitative results and discussions. Then extended theory is shown.

2. Transient Condensation of Deuteron Cluster

Since the meaningful enhancement of d–d fusion rate in steady state condition of deuterons trapped in metal lattice like PdDx is not possible [30], we have looked for dynamic conditions.

Using the implantation technique of low energy ion beam (deuteron, proton, and Si) from accelerators into titanium-deuteride (TiDx) plate-samples in vacuum, we have intensively searched if there exists any trace of deuteron cluster fusion [15,37–40,52], especially 3D (D + D + D) fusion which in conventional random motion or stochastic process of nuclear reaction should have very small reaction rate-ratio to d–d (D + D) fusion, [3D]/[2D] less than 10^{-30}. Namely, we should not observe any significant counts of produced particles (4.75 MeV t and 4.75 MeV ^{3}He, typically), according to the conventional theory of random nuclear reactions. On the contrary, our results [15,37–40] of beam implantation experiments provided very large data of [3D]/[2D] = about 10^{-4}, with increasing trend in low energy region less than 100 keV of D^+ beam energy. Namely, anomalous enhancement factor of about 10^{26}–10^{27} was obtained. To explain this with the beam-target reaction as conventional nuclear stochastic process, we need to assume the existence of close d–d pairs within 1 pm (10^{-12} m) inter-nuclear distance with 10^{-10} times population of deuterons in TiDx lattice. And experiments with proton beam [39,40] have suggested us that about half of three-body reactions (H + D + D or D + D + D) was due to the direct beam and close d–d pair reactions, and a remained half was attributed to the indirect (lattice-induced) three-body reactions that could be true deuteron cluster fusion. Therefore, to explain the enhancement factor of 10^{26}, we have sincerely to consider the mechanism of coherently induced cluster fusion in dynamic motion of TiDx and PdDx lattice.

Our preliminary model analyses were given in Refs. [30,31]; We adopted the excitation screening model. We have considered transient motion of deuterons at O-sites of PdDx lattice moving (diffusing) toward a T-site which is a candidate of focal points, for local full loading condition of PdDx, $x = 1.0$. This transient motion was conceived to be stimulated by exciting D-harmonic oscillators at O-sites near to the periodic trapping potential height of 0.22 eV.

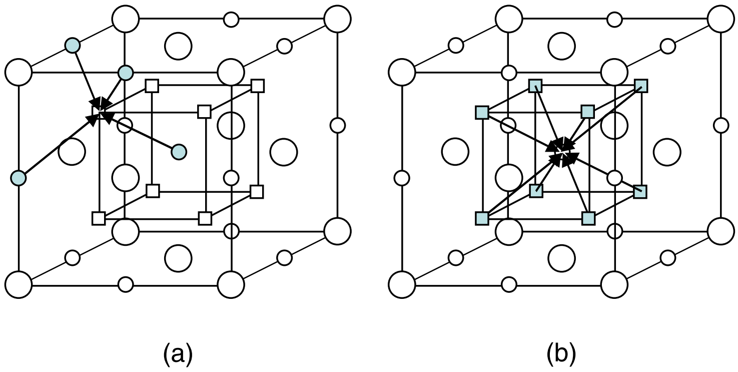

Figure 2. Tetrahedral condensation (a) and octahedral condensation (b); deuterons sit at octahedral sites for PdD and tetrahedral sites for PdD2 as local full or overloading condition.

Then cluster formation probabilities for 2D, 3D, and 4D "atomic" clusters were roughly evaluated, as shown in Fig. 1. This process of tetrahedral condensation is shown in Fig. 2a. This transient process of deuteron condensation at T-sites was considered [30,31] to be realized by squeezing many 4d-shell electrons of Pd atoms, which were quasi-free in the conduction band of Pd lattice. A two-dimensional view of this squeezing motion of deuterons and electrons into T-sites is shown in Fig. 3. Since many number of Pd atoms (more than eight), deuterons (four), and electrons (more than eight) are involved in this condensation process, an orthodox way of quantum mechanical treatment is to solve many coupled time-dependent Schroedinger equations with the potentials of three components, i.e., periodic atomic potential, Coulomb repulsive potential and nuclear strong interaction potential, in order to obtain deuteron cluster fusion rates. Of course this is a difficult task of computation.

For the treatment of zeroth order approximation, we adopted the model of strong coupling of phonons (D-harmonic oscillators) and 4d-shell electrons by D-plasma oscillation in PdDx lattice, and drew time-dependent behavior of periodic potentials which would have a transient deep potential hole (see Fig. 3 of Ref. [31]). We referred –80 eV for the depth of hole from Preparata's work [41]. In the next section, we will show the depth of hole is much deeper as –260 to –20 keV depending on the generation of transient Cooper-like pairs and/or quadruplet-coupling and octal coupling of electrons with anti-parallel spins. When a transient deep potential hole is born, e.g., four deuterons with four electrons are strongly attracted to the hole, namely at focal point (T-site in TRF case), and will accelerate to make a condensed cluster of deuterons within less than 1 pm-radius spherical domain. If we can calculate cluster fusion rates in a steady deep hole, we may convert it to time-averaged one, approximately by multiplying relative ratio of time-window for existence time of deep hole compared to plasma oscillation period, which is in the order of 10 fs. This is the way that we will extend the theory in the next section to make quantitative analysis. The EQPET model treat this by starting with assumption that total electronic wave function in transient deuteron cluster with electrons can be expanded by the linear combination of wave functions for transient molecular states like dde (namely $D_2{}^+$), ddee (D_2 molecule), dde* and dde*e* with transiently Bosonized electronic quasi-particle e* [48,49].

The INFN Frascati group of Celani et al. reported [42] very interesting and important results showing local superconductivity trend for over-D-loaded (D/Pd > 1) thin Pd wire in electrolysis. They reported resistance of wire became almost zero for 10–20 min interval and then quenched to normal resistance value of PdDx ($x = 0.7$). They also reported frequent observation of reduced resistance ratios R/R_0, probably showing tiny local superconductivity.

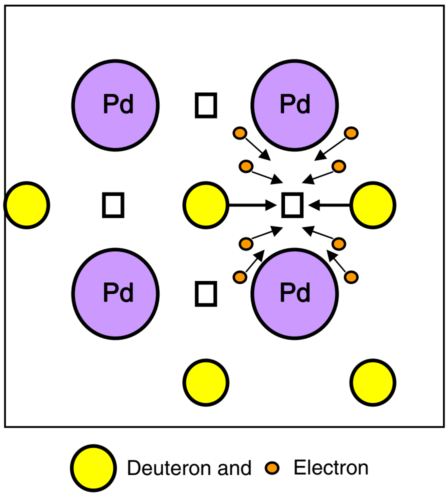

Figure 3. Squeezing of 4d-shell electrons (small circles) to focal point (T-site) of PdDx lattice.

Now we have to notify that PdDx is superconductivity material at low temperature less than 80 K, and over-D-loading ($x > 1$) will be the indication of the trend.

Recently Lanzara et al. published a paper in Nature [43] about observation of quasi-particle generation in high-T_c superconductor hole-doped copper-oxide, by means of angle resolved photo-electron emission spectroscopy. From two-peaked spectral data, they estimated about 1 ps lifetime for the electron quasi-particles (like Cooper pair). It is going to be clear that high-T_c superconductivity is induced by the generation of transient quasi-particle of electrons.

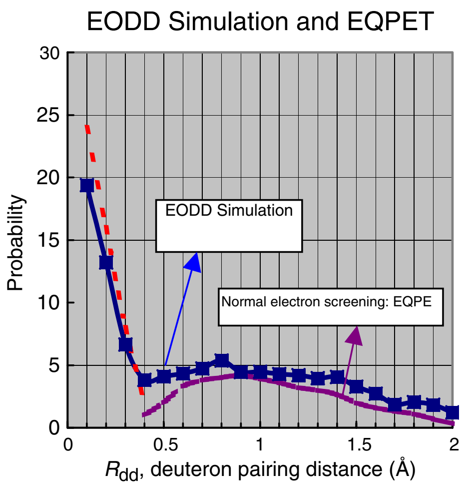

Figure 4. Transient electronic screening effects by EODD simulation [33] and EQPET [48], the lower R_{dd} component (broken line) is described by transient quasi-particle expansion.

This is anyway "transient bosonization" of electrons (fermions). We know that usually, the Pauli exclusion principle rules fermions (electrons) to block enhancement of screening of d–d Coulomb repulsive force. However, miracle of superconductivity may happen and the similar situation for generation of transient electronic quasi-particles will be true for deuteron fusion in condensed matter, by much localized transient bosonization, as we show in the next section.

The famous Japanese book of Solid State Physics [44] teaches us on superconductivity that: "behavior of charged particle in metal is well described by treating the interactions between plasma oscillation, phonons, free electrons, and shielded mutual interaction. Coupling between electron-system and phonon-system is the reason to generate superconductivity. Electron–electron interaction via phonon induces attractive force in the vicinity of Fermi surface, which compensates the shielded Coulomb repulsive force. The electron pair ($\mathbf{k}\uparrow, -\mathbf{k}\downarrow$), Cooper pair is selectively generated and annihilated in the strongly coupled state." The coherent range of Cooper pairs are regarded very long as greater than 100 nm for macroscopic superconductivity. We are going on the similar track for assuming electronic quasi-particles, but we are conceiving transient molecular states with single-particle-like e*. Two 1S- electrons in D_2 molecule have opposite spins in each other and mutual distance of electrons is about 0.1 nm. When one of electrons gets opposite momentum from outside interaction (for instance, by phonon–electron coupling and scattering in condensed matter), Two 1-S electrons may make a transiently Bosonized state (quasi-particle) with far less mutual distance than 0.1 nm and hence e* can be approximately treated as a single particle. So that, we do not necessarily require superconductivity condition in rather macroscopic domain, but do require localized microscopic order to generate transient electronic quasi-particle states with deuteron cluster.

Kirkinskii and Novikov [33] proposed the Electron Orbital Deformation Dynamics (EODD) model to treat the lattice dynamics in similar system as shown in Fig. 3. The EODD method is a kind of Monte–Carlo Molecular Dynamics calculation taking into account deformation of 5s + 4d shell electron-orbits by approach of two counter deuterons. They estimated the probability distribution of minimal pairing distances R_{dd} of deuterons, which showed a broadly peaked distribution in 0.5–2 Å region, probably reflecting minimum potential positions 1.1 and 0.7 Å, respectively, for dde and ddee (D_2) molecular states, and very interestingly steeply increasing component in lower R_{dd} region less than 0.2 Å as shown in Fig. 4. EODD simulation has given about 19% probability to have closely packed transient d–d pairs with less than 0.1 Å (even in 0.01 Å region) inter-nuclear distance which gives very enhanced fusion rate as 10^{-10} f/s/pair level [33]. It is regarded that this component realizes visible "cold fusion events." From our EQPET calculations [48] as reviewed in the next section, this component can be described as linear combination of Transient Electronic Quasi-Particle (TEQP) components, namely dde*(2,2), dde*(2,2), e*(2,2), dde*(4,4), and dde*(8,8), etc., as transient molecular states of EQPET theory [48]. This means that, when we will get three-dimensional EODD simulations for TRF and ORF systems, we will be able to fit the result with the combination of normal electron (dde + ddee) and transient quasi-particle screening (dde* + dde*e*) components. This should give the basis of EQPET.

3. EQPET Model

3.1. Basic Formulation

Some of MDx materials have been studied for high-temperature superconductivity trend, as typical significant effect was reported by Celani et al. [42] for full and over-loaded PdDx ($x = 1$ or > 1). The physics of low-temperature superconductivity is believed to be established by the BCS theory [50] and the physics of high-T_c (critical temperature) superconductivity has been studied, albeit not established yet, by extension of the BCS theory and Bogoliubov theory for electronic quasi-particle generation.

Deuteron at O-site (or T-site) in PdDx lattice behaves as an harmonic oscillator with phonon frequency ω_q. And motion of electrons is treated with plasma oscillation with frequency $\omega$of the lattice system with many electrons, deuterons and metal-atoms (e.g., Pd). By electron–phonon scattering, momentum $\mathbf{q} = \mathbf{k}–\mathbf{k}'$ is carried by phonon and two electrons having opposite momentum and spin may be born to generate a Cooper pair ($\mathbf{k}\downarrow$, $–\mathbf{k}\uparrow$) as an electronic quasi-particle, due to attractive force to compensate repulsive force of Coulomb interaction, in the phonon–electron coupled motion. Shielded Coulomb interaction potential is given [50] as:

$$V(q,\omega) = 4\pi e^2/(q^2 + k_s{}^2) + (4\pi e^2/(q^2 + k_s{}^2))(\omega_q{}^2/(\omega^2 - \omega_q{}^2)) \tag{3.1}$$

$$= (4\pi e^2/(q^2 + k_s{}^2))(\omega^2/(\omega^2 - \omega_q{}^2)), \tag{3.2}$$

where $1/k_s$ is the screening distance for Fermi gas. The first term of Eq. (3.1) shows normal Coulomb repulsive potential between electrons, and the second term shows phonon-mediated interaction. As clearly seen by Eq. (3.2), the potential becomes negative (attractive) if $\omega < \omega_q$. This is a driving force to produce Cooper pairs. When two deuterons with electrons are squeezing from opposite directions to T-site (or O-site) under the TRF (or ORF) transient condensation [51], the condition of opposite momentum and spin for two electrons can be naturally fulfilled (see Fig. 3). However, directions of deuterons in TRF and ORF condensation are not ideally 180° opposite, so that momentum transfer by phonon-electron coupling makes conditioning for transient Cooper-like pairs. Actually, quasi-particle state may be generated by formation of orthogonally coupled two D_2 molecules to associate electronic quadruplet, as we show in Section 4.

Effective mass m^* and effective charge e^* of Cooper-like pair can be approximately given [50] as $m^* = 2m_e$ and $e^* = 2e$. Microscopic Cooper-like pair with short life around lattice focal point can be regarded as single particle, as discussed, with mass $2m_e$ and charge $2e$. Hence we label Cooper-like pair as $e^*(m^*/m_e, e^*/e) = e^*(2,2)$. Cooper-like pair is the s-wave pairing of two electrons with opposite momentum and spin. To explain high-Tc superconductivity, generation of unconventional pairing (e.g., d-wave pairing) and very heavy fermions (several hundred times mass of electron) have been proposed (see Chapter 9 of Ref. [50]), albeit reaching no consensus yet. By considering higher order pairing (s-wave) of binary e*(2,2) quasi-particles to generate a quadruplet-coupling e*(4,4) and moreover octal coupling e*(8,8) by binary e*(4,4) quasi-particles, we may treat the state of high-T_c superconductivity, instead of assuming heavy fermions (electrons), as we see later. "Bosonized" electron wave function Ψ_N for N-electrons system in MDx lattice will be approximated, as discussed in the previous section, by a linear combination of normal electron wave function $\Psi_{(1,1)G}$ and quasi-particle wave functions $\Psi_{(2,2)G}$, $\Psi_{(4,4)G}$, and $\Psi_{(8,8)G}$ as;

$$|\Psi_N\rangle = a_1|\Psi_{(1,1)G}\rangle + a_2|\Psi_{(2,2)G}\rangle + a_4|\Psi_{(4,4)G}\rangle + a_8|\Psi_{(8,8)G}\rangle. \tag{3.3}$$

Here we consider each wave function is further a linear combination of wave functions for single and double electrons or e^*. This may be called the quasi-particle expansion of total electronic wave function. Here suffix G denotes ground state. For MDx system, the normal electron wave function $|\Psi_{(1,1)G}\rangle$ coupled with phonon may be given by a Bloch function with lattice period x_l, combined with harmonic oscillator motion for D, in one-dimensional case; Using Hermite polynomial H_n,

$$|\Psi_{(1,1)G}\rangle = \sum C_l \exp(\mathrm{il}(x - x_l)) \sum \exp(-\alpha_n (x - x_l)^2) H_n{}^2(\alpha_n{}^{1/2}(x - x_l)). \tag{3.4}$$

The ground state BCS wave function is defined as,

$$a_1|\Psi_{(1,1)G}\rangle + a_2|\Psi_{(2,2)G}\rangle = \prod (u_k + v_k C^*_{k\uparrow} C_{-k\downarrow}|\Psi_0\rangle, \tag{3.5}$$

where $|\Psi_0\rangle$ denotes vacuum, u_k is the un-occupied wave function of Cooper-like pair and v_k is the occupied wave function of Cooper-like pair; hence $u_k{}^2 + v_k{}^2 = 1$ is the normalization condition. $C^*{}_{k\uparrow}$ and $C_{-k\downarrow}$ are generation and destruction operators, respectively.

We may define production operator $C^*{}_{2\mathrm{k}}$ and destruction operator $C_{2\mathrm{k}}$ for bosonized (spin zero) e*(2,2) to generate quadruplet-coupling e*(4,4) as,

$$a_1|\Psi_{(1,1)\mathrm{G}}\rangle + a_2|\Psi_{(2,2)\mathrm{G}}\rangle + a_4|\Psi_{(4,4)\mathrm{G}}\rangle = \prod(u_{2\mathrm{k}} + v_{2\mathrm{k}}C^*{}_{2\mathrm{k}}C_{2\mathrm{k}})|\Psi_0\rangle \tag{3.6}$$

with $u_{2\mathrm{k}}{}^2 + v_{2\mathrm{k}}{}^2 = 1$ for normalization. Wave function for e*(8,8) is similarly defined.

To evaluate coefficients a_1, a_2, a_4, and a_8, we may apply the variational method with evaluating the BCS Hamiltonian (see Chapter 3 of Ref. [50]);

$$H = \Sigma\Sigma\varepsilon_\mathrm{k} n_{\mathrm{k}\sigma} + \Sigma\Sigma V_{\mathrm{kl}} C^*{}_{\mathrm{k}\uparrow} C^*_{-\mathrm{k}\downarrow} C_{-\mathrm{l}\downarrow} C_{\mathrm{l}\uparrow} \tag{3.7}$$

and

$$\delta\langle\Psi_N{}^*|H|\Psi_N\rangle = 0. \tag{3.8}$$

The above equations are just for formality, and we need further extension to substantiate the problem. However, essential components of the problem can be analyzed as follows.

3.2. Screening Effect and Fusion Rates

For the time-window of potential deep hole [31,51], effective (time-averaged) screening potential, for a d–d pair in a transient D-cluster of 4–8 deuterons for TRF and ORF condition [51], can be defined by a screened potential of quasi-particle complex;

$$V_\mathrm{s}(R) = b_1 V_{\mathrm{s}(1,1)}(R) + b_2 V_{\mathrm{s}(2,2)}(R) + b_4 V_{\mathrm{s}(4,4)}(R) + b_8 V_{\mathrm{s}(8,8)}(R). \tag{3.9}$$

Here R is the inter-nuclear distance of a d–d pair and $V_\mathrm{s}(m^*/m_\mathrm{e}, e^*/e)(R)$ is the screened potential for a dde($m^*/m_\mathrm{e}, e^*/e$) molecule, for $(m^*/m_\mathrm{e}, e^*/e)$ = (1,1), (2,2), (4,4), and (8,8). Time-averaging treatment for transient D-cluster condensation with electrons including transient quasi-particles is transferred here to coefficients b_1–b_8. By definition, we need to satisfy the following normalization condition.

$$b_1{}^2 + b_2{}^2 + b_4{}^2 + b_8{}^2 = 1. \tag{3.10}$$

For a dde or dde* molecule (one quasi-particle approximation) within the short time-interval of D-clustering, wave function of a d–d pair (2D) is given by the solution of the following Schroedinger equation:

$$(-h^2/8\pi\mu)\nabla^2 X(R) + (V_\mathrm{n}(R) + V_\mathrm{s}(R))X(R) = EX(R) \tag{3.11}$$

with nuclear potential $V_\mathrm{n}(R)$ for strong interaction and reduced deuteron mass μ.

By Born–Oppenheimer approximation, we assume as,

$$X(R) = X_\mathrm{n}(R)X_\mathrm{s}(R). \tag{3.12}$$

Overlapping rate of $X(R)$ at $R = r_0$ gives estimation of d–d fusion rate $\lambda_{2\mathrm{d}}$ as:

$$\begin{aligned}\lambda_{2\mathrm{d}} &= G|X(R)|^2{}_{R=r_0} \\ &= G|X_\mathrm{n}(R)|^2{}_{R=r_0}|X_\mathrm{s}(R)|^2{}_{R=r_0},\end{aligned} \tag{3.13}$$

where G is the scaling constant and r_0 is given to be 5 fm considering deuteron radius plus charged-pion exchange range (about 2 fm) at contact surface configuration of the moment of strong interaction for d–d fusion reaction.

Using WKB approximation for the barrier ($V_s(R)$) penetration probability,

$$|X_s(R)|^2{}_{R=r_0} = \exp(-2\Gamma_n(E_d)); \qquad \text{Barrier Factor (BF)}, \tag{3.14}$$

where E_d is the relative deuteron energy and Γ_n is Gamow integral for a d–d pair in D-cluster (n-deuterons with electrons) that is defined as:

$$\Gamma_n(E_d) = (2\mu)^{1/2}/(h/\pi)\int_{r_0}^{b}(V_s(R) - E_d)^{1/2}\mathrm{d}R. \tag{3.15}$$

Using astrophysical S-factor for strong interaction,

$$\mathrm{G}|X_n(R)|^2{}_{R=r_0} = \mathrm{vS_{2d}}(E_d)/E_d. \tag{3.16}$$

Consequently we can approximately define tow-body fusion rate as:

$$\lambda_{2d} = (\mathrm{vS_{2d}}(E_d)/E_d)\exp(-2\Gamma_n(E_d)). \tag{3.17}$$

We can estimate Gamow integral for dde* molecule, by solving Schroedinger equation to obtain screened potential $V_s(m^*/m_e, e^*/e)$ and evaluate the corresponding Gamow integral $\Gamma_n(m^*/m_e, e^*/e)$ by, for each electron and quasi-particle molecular state,

$$\Gamma_{n(m^*/m_e,e^*/e)}(E_d) = (2\mu)^{1/2}/(h/\pi)\int_{r_0}^{b}(V_{s(m^*/m_e,e^*/e)}(R) - E_d)^{1/2}\mathrm{d}(R). \tag{3.18}$$

Using Eqs. (3.15) and (3.9) with condition of $V_s(R) \gg E_d$; $R < b$, and considering that b-parameter becomes independent own value for each quasi-particle, we can approximately obtain:

$$\Gamma_n(E_d) = b_1\Gamma_{n(1,1)}(E_d) + b_2\Gamma_{n(2,2)}(E_d) + b_4\Gamma_{n(4,4)}(E_d) + b_8\Gamma_{n(8,8)}(E_d). \tag{3.19}$$

To estimate coefficients $b_1 - b_8$, we have to solve coupled channel Schroedinger equations of normal electrons, Cooper pairs, quadru-couplings, e*(8,8) by Eqs. (3.3)–(3.8), to evaluate first relative state densities of a_1–a_8. This is a hard task to do in future. For some simplified cases as in Section 4, we have estimation.

Screened potentials $V_s\mathrm{n}(m^*/m_e, e^*/e)(R)$ were calculated for dde* molecular states using extended solutions for dde state given in a text of quantum mechanics by the well-known technique of variational method [45] as:

$$V_{s(m^*/m_e,e^*/e)}(R) = V_h + e^2/R + (J + K)/(1 + \Delta), \tag{3.20}$$

where the Coulomb integral J, the exchange integral K, and the non-orthogonal integral Δ are given as [45]:

$$J = Z(e^2/a)[-1/y + (1 + 1/y)\exp(-2y)], \tag{3.21}$$

$$K = -Z(e^2/a)(1 + y)\exp(-y), \tag{3.22}$$

$$\Delta = (1 + y + y^2/3)\exp(-y). \tag{3.23}$$

With

$$Y = R/a, \tag{3.24}$$

$$a = a_0/Z/(m^*/m_e) \tag{3.25}$$

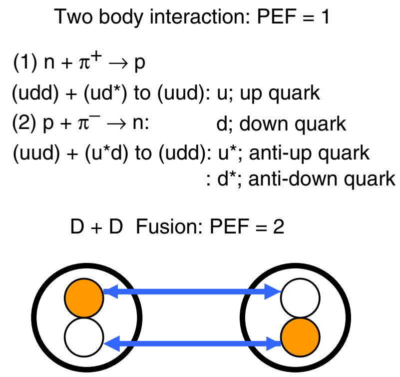

Figure 5. PEF factor to scale strong interaction for nuclear fusion.

with a_0= 0.053 nm (Bohr radius) and $Z = e^*/e$.

We also solved an atomic de* system to obtain ground state energy $V_\mathrm{h}$as:

$$V_\mathrm{h} = -13.6Z^2/(m_\mathrm{e}/m^*). \tag{3.26}$$

For dde*e* molecule state with double electrons or e* s, we also extend the solution for ddee given in the text [45] and we have obtained screened potential function $V_{\mathrm{se^*e^*}}$ as:

$$V_{\mathrm{se^*e^*}}(R) = 2V_\mathrm{h} + e^2/R + (2J + J' + 2\Delta K + K')/(1 + \Delta^2). \tag{3.27}$$

Here the cross-Coulomb integral J' and cross exchange integral K' are given as:

$$J' = (Z^2e^2/a)(1/y - \exp(-2y))(1/y + 11/8 + 3y/4 + y^2/6), \tag{3.28}$$

$$\begin{aligned} K' = (Z^2e^2/5/a)[&-\exp(-2y)(-25/8 + 23y/4 + 3y^2 + y^3/3) \\ &+(y/6)((0.5772 + \log y)\Delta^2 \\ &+(\Delta')^2 E_\mathrm{i}(-4y) - 2\Delta\Delta' E_\mathrm{i}(-2y))] \end{aligned} \tag{3.29}$$

with

$$\Delta' = \exp(-y)(1 - y + y^2/3), \tag{3.30}$$

$$E_\mathrm{i}(y) = -\int_0^{\exp(-y)} (1/\log x)\, \mathrm{d}x. \tag{3.31}$$

We should note here that in these equations corrections were made for mistakes in the text book [45].

For fusion rates of multi-body (nD) reactions in a D-cluster was defined [51] as:

$$\lambda_\mathrm{nd} = [vS_\mathrm{nd}(E_\mathrm{d})/E_\mathrm{d}]\exp(-n\Gamma_\mathrm{n}(E_\mathrm{d})). \tag{3.32}$$

Here we have assumed that a simultaneous multi-body fusion process can be approximately treated by the very fast sequential process, e.g. (D + (D + (D + D))) of cascade two-body reactions for intermediate states [51]. And we have made estimate for $S_\mathrm{nd}(0)$ values by using empirical scaling of known $S(0)$-values of H + D, D + D, and D + T fusion

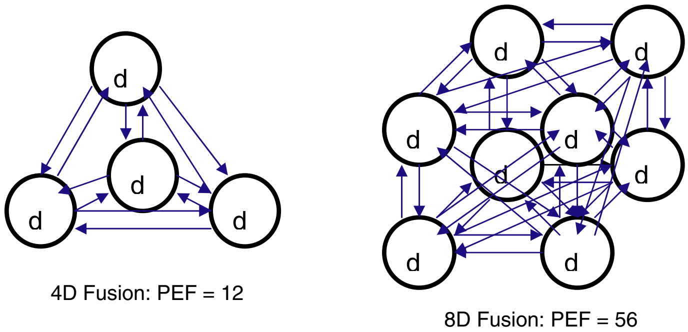

Figure 6. Charged pion exchange for 4D TRF and 8D ORF condensations.

reactions extrapolating up to unknown multi-body $S_{\rm nd}(0)$ values as a function of pion exchange force (PEF) numbers for equilaterally symmetric configuration of strong interaction (Π^+ and Π^- exchange) in TRF and ORF condensation [51]. The second term of Eq. (32) gives multi-body barrier factor.

3.3. TRF-and ORF-Resonance of Strong Interaction

To make an empirical scaling law of effective S-values (astrophysical S-values) for two-body and multi-body deuteron-related fusion cross-sections, PEF parameter which is a relative measure of contact surface area of pion exchange has been defined [17,30,31,32]. The larger is the contact surface area, the larger is fusion cross section. The basic idea is illustrated in Fig. 5. Since the neutral pion exchange corresponds to scattering process between nucleons, exchange of charged pions (positive and negative) is regarded to be attributed to nuclear fusion. Single charged pion exchange between neutron and proton is defined as PEF = 1 as scaling factor of fusion-strong-interaction. By using quarks instead of pions, we obtain same results. So, we can evaluate degree of strong interaction for fusion by using charged pion exchange (Yukawa model). Using this relative PEF unit, pion exchange for D + D fusion is counted as PEF = 2. We extend the idea to others and obtain PEF = 3 for D + T, PEF = 6 for D + D + D (3D), PEF = 12 for 4D, and PEF = 56 for 8D, as illustrated interactions for 4D equilateral tetrahedron and 8D equilateral octahedron (deuteron site at face-center)

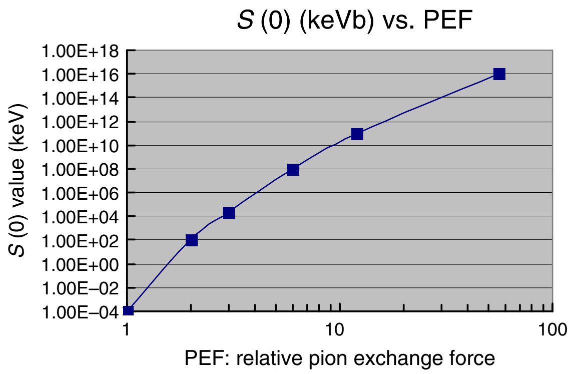

Figure 7. Speculative extrapolation of effective S-values for multi-body fusion.

in Fig. 6. TRF condensation can realize equilaterally tetrahedral configuration in charged pion exchange with same inter-deuteron distance for each deuteron: namely best condition to enhance effective contact surface of pion cloud to form virtual compound ^{8}Be* as intermediate fusion product which breaks up shortly to two α-particles. Equilateral triangle configuration for 3D fusion is next good.

For deuteron clusters of 5D, 6D, and 7D, symmetric pion-exchange condition is geometrically so violated that local 4D cluster-component may have geometrically symmetric tetrahedral configuration and resultantly 4D fusion becomes selective. For 8D cluster, symmetric condition recovers: however, interaction distances are identical and shorter to three neighboring deuterons, but identical and longer to remained four deuterons. Therefore, PEF = 56 for 8D fusion is considerably overestimation: this may mean that degree of strong interaction for fusion should be saturated for high number of nucleons. This looks true when we see changing trend of S-values of reactions between deuteron and higher mass-nuclei (^{6}Li,^{10}Be,^{12}C, and so on). However intrinsic difference, for example, between d + ^{6}Li fusion and TRF 4D fusion (both produces intermediate virtual compound ^{8}Be*) is that about half (3) of nucleons (neutron and proton) of ^{6}Li nucleus sphere are shielded with other half (3) of nucleons to make direct charged pion exchange in contact surface, while TRF 4D fusion realizes completely symmetric exchange without shielding affect. Because of above-discussed reason, we can expect resonantly strong enhancement of fusion cross sections (effectively S-values) for 3D, 4D, and 8D fusion. In addition, because of high PEF values, 4D TRF and 8D ORF may have strongest "resonance" condition. We may say that 3, 4, and 8 are "magic numbers" for deuteron cluster fusion.

Using thus counted PEF values for scaling parameter, we have obtained extrapolated S-value plot for 4D TRF and 8D ORF reactions based on known S-values of H + D, D + D, and D + T reactions, as shown in Fig. 7. We have obtained rough values of 10^{12} keV barn for 4D TRF and 10^{16} keV barn for 8D ORF, which are extremely large values compared to those of conventional two-body fusion.

Using Eq. (3.32) with estimated S-values and BF values, we have got fusion rates per cluster for 2D, 3D, 4D, and 8D fusion. Results (Table 1) will be shown in the next section.

3.4. Numerical Results and Discussions

We have done calculations of screening potentials of dde* and dde*e* molecules with heavy electrons (fermions) for $m^* = 1m_e$ to $208m_e$ (muon), to make comparison with screening effects by quasi-particles of e*(2,2), e*(4,4), and e*(8,8).

Figure 8 shows the effect of first-step bosonization, namely generation of Cooper-like pair, compared with screened potential of D_2 molecule (ddee system) which has minimum transient potential hole (–10.6 eV) at $R_e = 0.07$ nm. Value

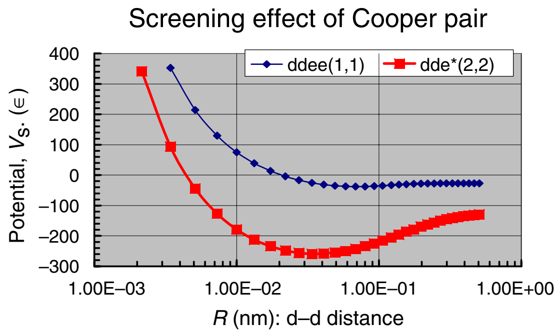

Figure 8. Screening effect of Cooper-like pair for dde* molecule, compared with D_2 molecule.

Table 1. Barrier-Factors (BF) and Fusion-Rates (FR in f/s/cl), by transient quasi-particle screening

$(m^*/m_e, e^*/e)$	2D BF (FR)	3D BF (FR)	4D BF (FR)	8D BF (FR)
(1,1)	10^{-125} (10^{-137})	10^{-187} (10^{-193})	10^{-250} (10^{-252})	10^{-500} (10^{-499})
(2,1)	10^{-53} (10^{-65})	10^{-80} (10^{-86})	10^{-106} (10^{-108})	10^{-212} (10^{-211})
(2,2)	10^{-7} (10^{-20})	10^{-11} (10^{-17})	10^{-15} (10^{-17})	10^{-30} (10^{-29})
(4,4)	3×10^{-4} (3×10^{-16})	10^{-5} (10^{-11})	10^{-7} (10^{-9})	10^{-14} (10^{-13})
(4,4)b	4×10^{-1} (4×10^{-13})	2×10^{-1} (2×10^{-7})	10^{-1} (10^{-3})	2×10^{-2} (2×10^{-1})

of b-parameter for Gamow integral is approximately given by the zero-potential crossing distance; which is essential to barrier penetration calculation. Value of b-parameter moves from 20 pm for D_2 molecule to 4 pm for dde*(2,2) Cooper-like pair. This is drastic effect: as given in Table 1, barrier factor increases from 10^{-50} with $\lambda_{2d} = 10^{-63}$, for D_2, to 10^{-7} with $\lambda_{2d} = 10^{-20}$, for Cooper-like pair dde*. Assuming macroscopic production density of 10^{20} (1% of D-density in PdDx, $x > 1$) Cooper-like-pairs/cm^3, we obtain D + D (2D) fusion yield of 1 f/s/cm^3, that is, so called Jones level and lowest countable level by usual neutron detectors. We can say that Cooper-like pair can make great effect to drastically enhance d–d fusion rate in MDx systems. This may be the first clear theoretical evidence that "cold fusion" exists. Cooper-like pair generates transient deep hole (–256 eV) to attract deuterons and initiate D-cluster condensation [51].

In Fig. 9**,** dde* potentials are compared between Cooper-like pair e*(2,2) and a heavy fermion e*(10,1). Screening effects are comparable. In Fig. 10, comparison is also made for quasi-particle of quadruplet-coupling e*(4,4) and very heavy fermion e*(100,1), to show comparable effects between the two.

Where $E_d = 0.22$ eV is assumed, which is the $n = 3$ phonon excited state of D in PdDx lattice with $h\omega_0 = 64$ meV and $E_d = (n+1/2)h\omega_0$. And (0,0): bare dd reaction, (1,1): dde- molecule, (2,1): dde* with heavy electron, (2,2): dde* with Cooper pairing, (4,4): dde* with quadru-coupled electrons, (4,4)b: dde* with binary quadru-coupled electrons, namely (8,8)

Muon has $m^* = 208m_e$, so that binary Cooper-like coupling, namely quadruplet-coupling e*(4,4) works as strongly as muon for D + D fusion induction. We can say that the very heavy fermion model for high-T_c superconductivity can be replaced with the binary bosonization of two Cooper pairs to make e*(4,4) quadruplet-coupling. Depth of the transient deep hole [45,51] by e*(4,4) generation is so large as –2460 eV, that can strongly attract surrounding deuterons

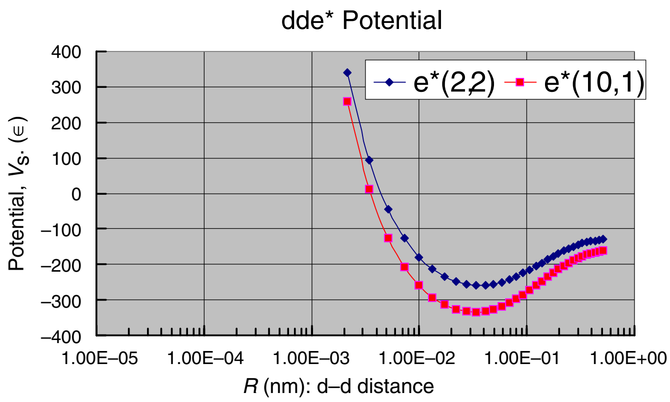

Figure 9. Comparison of screened potentials between Cooper-like pair and mass-10 heavy fermion..

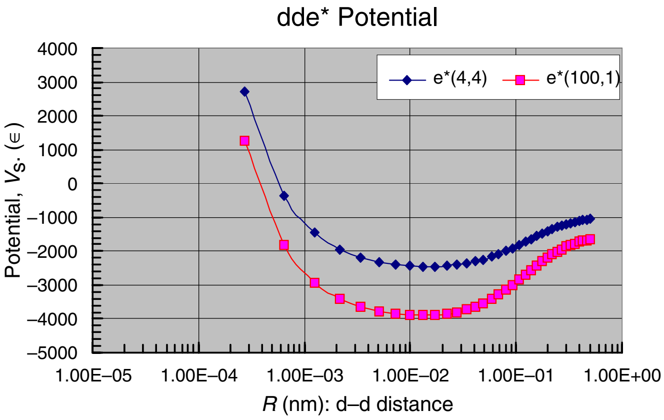

Figure 10. Comparison of screened potentials between e*(4,4) quasi-particle and mass-100 heavy fermion.

with electrons to make TRF and ORF condensations at focal points. Value of b-parameter for dde*(4,4) is about 0.5 pm (500 fm), to enhance D + D barrier factor to 3×10^{-4}, and 10^{-5} for 3D and 10^{-7} for 4D multi-body fusion, of which fusion rates (microscopic) are 10^{-16}, 10^{-11}, and 10^{-9}, respectively, for 2D, 3D, and 4D fusion. If we assume D-cluster density of 10^{20} cl/cm^3, we obtain fusion yield (f/s/cm^3) of 10^4, 10^9, and 10^{11}, respectively, for 2D, 3D, and 4D fusion, which are already "miracle" values to meet with major claims of "cold fusion" experiments. 8D fusion yield becomes significant level as 10^7 f/s/cm^3.

Figure 11 shows the bosonization effect of binary e*(4,4) quasi-particles, namely octal-coupling e*(8,8). When this extreme condition is realized as ORF (see Section 4), we have b-parameter of 70 fm within which domain deuterons can approach as classical particles to make very condensed D-cluster for very enhanced strong interaction between 3, 4, and 8 resonant deuterons [49,51] simultaneously (within Heisenberg uncertainty) as previously discussed. This screening effect of binary e*(4,4)b, namely e*(8,8) is comparable to that of heavy fermion e*(300,1). Depth of transient deep hole by e*(8,8) is very large as –20.6 keV. When we recall that the first-step goal of DT plasma temperature in TOKAMAK device is around 10 keV, e*(8,8) can provide comparable "acceleration condition," however microscopically "coherent" way. Thus, 8D fusion can be winner of D-cluster fusion as discussed previously [48,51]. 8D fusion emits two high-energy (47.6 MeV) ^{8}Be-particles, which can induce secondary capture reactions to make transmutation with mass-8 and charge-4 increment, as recently claimed by MHI experiment [27].

3.5. Discussions for Nuclear Products

In the TRF or ORF condensation process, we conceive that there happens a competing process of d + d and multi-body deuteron fusion reactions as follows.

(1) 2D → n + ^{3}He + 3.25 MeV, p + T + 4.02 MeV,
(2) 3D → Li^{6*} → t + He^3 + 9.5 MeV,
(3) 4D → Be^{8*} → 2 × He^4 + 47.6 MeV,
(4) 5D → B^{10*} (53.7 MeV),
(5) 6D → C^{12*} (75.73 MeV),
(6) 7D → N^{14*} (89.08 MeV),
(7) 8D → O^{16*} (109.84 MeV) → 2 × Be^8 + 95.2 MeV.

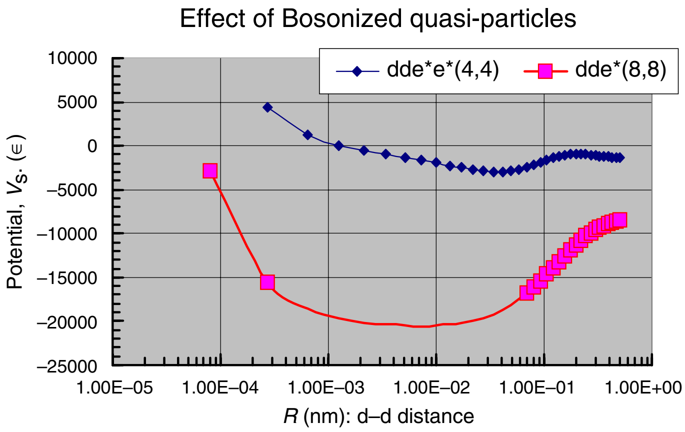

Figure 11. Bosonization effect of e*(4,4) binary quasi-particles, on screened potential.

Nuclear products of 4D fusion was discussed in detail in Ref. [31]. Here we simply assume that two ^{4}He (α-particles) with 23.8 MeV kinetic energy emit into 180° opposite directions each other, and slow down in PdDx lattice by ionization and knock-on process. 23.8 MeV α-particle has very small cross section to ionize K-shell electrons of Pd (therefore there are no emission of K-X-rays of about 22 keV), but has considerable cross sections for L-and M-shell electrons (therefore we see small component of L-and M-X-rays in several keV region). Largest component of X-rays in continuous region less than 3.5 keV is attributed to slowing down of convey electrons by α-particles.

Possible nuclear product of 8D fusion via intermediate virtual excited state of ^{16}O* is shown in Table 2. There are so many exit channels. However, we conceive only two channels are predominant. ^{16}O is a typical α-clustered nucleus. Ground state of ^{16}O is composed of four equilaterally tetrahedral α-particles in combination, and at highly excited state in collective oscillation the nucleus is deformed into two cases; (1) deformation with two ^{8}Be particles, or (2) deformation with

α-Particle and ^{12}C nucleus. Emitted ^{8}Be particles by 8D fusion have very high-kinetic energy of 47.6 MeV which is well over Coulomb barrier height of interaction with neighboring heavier nuclei to make secondary nuclear reaction as capture and fission. ^{8}Be has very short life time as 6.7×10^{-17} s and decays shortly to two ^{4}He, but has enough time to make several interactions with neighboring nuclei in the range.

Nuclear products from 3D fusion were already discussed in other reports [30,31]. 2D and 3D fusion may become minor branches in TRF and ORF deuteron-cluster condensations. This situation is quite in contrast to conventional stochastic two-body fusion reactions. Electron quasi-particles and multi-body resonance fusion play miracle role in condensed matter, which contain fully deuterons and resultantly may induce local superconductivity.

3.6. Explanation to Key Experimental Claims

Explanation to ^{4}He major products in correlation with excess heat has been already mentioned in the above discussions. The reason why we see very scarce neutrons in "cold fusion" experiments is also clear by the competition story of 2D, 3D, 4D and 8D fusion rates since 4D and 8D fusion can be winner of the competition under the strong screening and attraction by transient electronic quasi-particle generation.

The extraordinary result [24–26] of Iwamura et al. reporting mass-8-and-charge-4 increased transmutation is now on discussion. On surface of thin Pd layer they made deposit of thin test element (Sr or Cs). Back side of supporting thick

Table 2. Decay channels of 8D fusion

8D → $^{16}O^*$	
	→ n + ^{15}O + 94.16 MeV
	→ p + ^{15}N + 97.70 MeV
	→ d + ^{14}N + 89.09 MeV
	→ t + ^{13}N + 84.79 MeV
	→ ^{3}He + ^{13}C + 87.03 MeV
	→ ^{4}He + ^{12}C + 102.66 MeV
	→ ^{6}Li + ^{10}B + 78.95 MeV
	→ ^{7}Li + $^{9}B^*$ + 77.76 MeV
	→ $^{7}Be^*$ + ^{9}Be + 77.97 MeV
	→ $^{8}Be^*$ + $^{8}Be^*$ + 95.2 MeV

(0.1 mm) Pd zone was evacuated, and front side of film was filled with D_2 gas. They realized constant D-permeation (1 cm^3/min) through the multi-layered film, which would keep over-loading condition PdDx ($x > 1$) within the first thin zone of Pd, which is thought to be reaction-active zone. They observed the transmutation only in the case of existing CaO layer with D-flow; In cases of H-flow with CaO and D-flow without CaO, they observed no transmutation.

CaO zone enlarges gap of electron Fermi levels in the interface region of Pd and CaO, and same thing may happen in the interface of Pd and Sr or Cs test zone. Enlarged Fermi level gaps may help increase movement of free electrons which will enhance generation of Cooper-like pair or quadruplet-coupling of electrons, i.e., transient bosonization of electrons which would play drastic role of inducing deep potential holes to attract deuteron-clusters with electrons at focal points of T- and O-sites of regular PdDx lattice and some defect points in the interface. Local D-over-loading would have been generated. 4D TRF and 8D ORF, especially the latter was induced there to produce high energy ^{8}Be particles which would be captured by neighboring heavier nuclei as Sr or Cs to make the following transmutation reaction;

$$M(A, Z) + {}^{8}\mathrm{Be}\,(47.6\ \mathrm{MeV}) \to M(A+8, Z+4)^*(Ex) + KE. \quad (3.33)$$

A cartoon illustration of reactions is shown in Fig. 12. Since ^{8}Be particle with short life (unstable) is thought to be highly deformed as illustrated, we expect enhanced capture cross section by large contact surface exchanging charged pions with target heavy nucleus.

Coulomb barrier heights for reaction (3.33) are 22.5 MeV for M = Sr, and 30.1 MeV for M = Cs, which were calculated using effective contact distance for fusion as $R_f = R_1 + R_2 + \lambda$ with pion wave length λ, $R_1 = 1.2A_1^{1/3}$, $R_2 = 1.2{A_2}^{1/3}$. Possible products of reaction (3.33) for Sr and Cs are shown in Table 3. Excited energy E_x of

Table 3. Products of Be^8 absorption reaction

(1) ^{88}Sr + ^{8}Be (47.6 MeV) → ^{96}Mo*(53.43 MeV)	
	→ ^{96}Mo($Ex.$)* + KE (deposit to lattice) or FP1 + FP2 + Energy :fission (many channels)
(2)^{133}Cs + ^{8}Be (47.6 MeV) → ^{141}Pr*(50.47 MeV)	
	→ ^{141}Pr(Ex)* + KE (deposit to lattice) or FP1 + FP2 + Energy :fission (many channels)

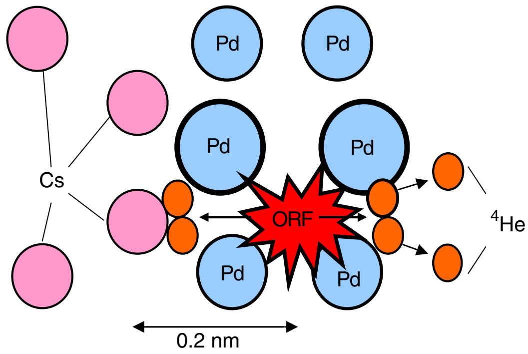

Figure 12. An imagination of 8D fusion and Be^8 capture.

intermediate compound nucleus Mo*(or Pr*) may distribute from 53.43 MeV (50.47 MeV for Pr) to 4.8 MeV (2.9 MeV for Pr) depending on the transferred energy to kinetic energy KE. Imagining liquid-drop like collision character of the reactions (3.33), most energy will be transferred to KE (Mo or Pr kinetic energy), which will make deposit to lattice vibration by heavy particle slowing down in condensed matter without emitting hard and soft X-rays. Thus, major part of experimental results can be explained by the present model. However, when E_x can be large enough to be over fission barrier (about 20 MeV for Mo, and 15 MeV for Pr), distributed mass- and Z-products may be produced. As a function of E_x, fission products distribution can be estimated by the selective channel scission theory [46,47]. Therefore, we need to know data of energy sharing between E_x and KE for reaction (3.33). This is unresolved problem and further study is expected.

4. Further Extension of EQPET Model

4.1. Deuteron Cluster Fusion

Model example of deuteron cluster fusion was proposed as the Tetrahedral Symmetric Condensation (TSC) and the Octahedral Symmetric Condensation (OSC) in PdDx lattice dynamics. As illustrated in Fig. 2, TSC may take place at locally full loaded PdD regions ($x = 1.0$), while OSC may happen much more difficultly at locally overloaded PdD_2 regions ($x = 2.0$). As discussed later on power level, we only need to require local density of 10^{-6} times (ppm order) of Pd density for the OSC condition, while much higher local density, e.g., 10% of Pd atomic density is required for the TSC condition. To generate electronic quasi-particle states, basic mechanism is thought to be the dynamic formation of quadruplet deuteron molecule, which is an *orthogonal coupling of two* D_2 *molecules*, as illustrated in Fig.13.

Three-dimensional motion of TSC can be converted to two-dimensional motion using momentum vector conversion [62]. A two-dimensional view of TSC is shown in Fig. 14. To minimize total energy of the system, charge neutral condensation in average of 4D cluster (four deuterons with alternately coupled four electrons with anti-parallel spins for counter-part electrons with reversed momentums) may cause the central point (T-site in this case) condensation from 4 O-sites of deuterons and 4-sites of electrons. Hence, transient condensate of electrons, namely quadruplet e*(4,4) may be formed at around the central T-site.

We assume a similar condition for the OSC motion, as illustrated in Fig. 15. When four electrons down-spins are happening to be arranged on upper half together with four electrons up-spins on lower half, averaged charge neutral condensation from 8 T-sites to the central O-site may become possible, to form 8D cluster with an octal-coupling state e*(8,8) of electrons at around the central O-site. This condition may realize super-screening for

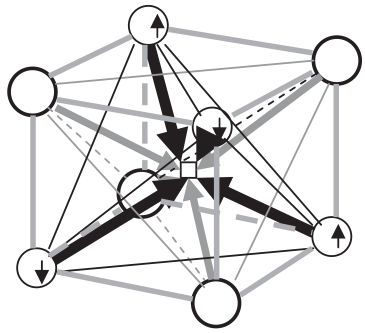

Figure 13. TSC, bigger circles for deuterons and smaller circles with arrow (spin) for electrons.

virtual d-d pairs in the 8D cluster, and 8D fusion rate can be calculated by the rapid cascade reaction model, i.e., D+(D+(D+(D+(D+(D+(D + D)))))) [60,62].

4.2. Advanced EQPET Model

A 4D cluster under TSC condition will cause 2D, 3D, and 4D nuclear fusion in competition, because the TSC state reflects the atomic level motion of deuterons in condensed matter and does not necessarily relate to 4D nuclear fusion reaction as strong interaction. In the same way, an 8D cluster causes the competition process of nuclear fusion reactions between 2D, 3D, 4D and 8D nuclear fusion reactions. We need therefore to define and estimate modal fusion rates to TSC and OSC processes [60]. Modal fusion rates are defined as:

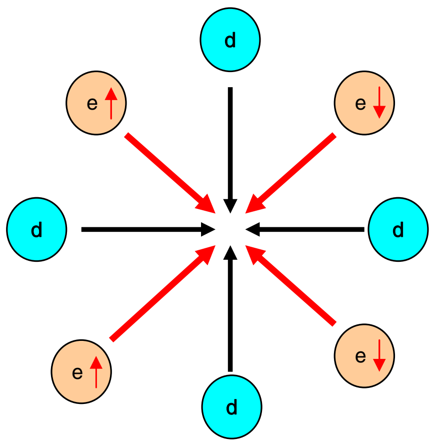

Figure 14. Two-dimensional view of TSC, plus charge for d, minus charge for e.

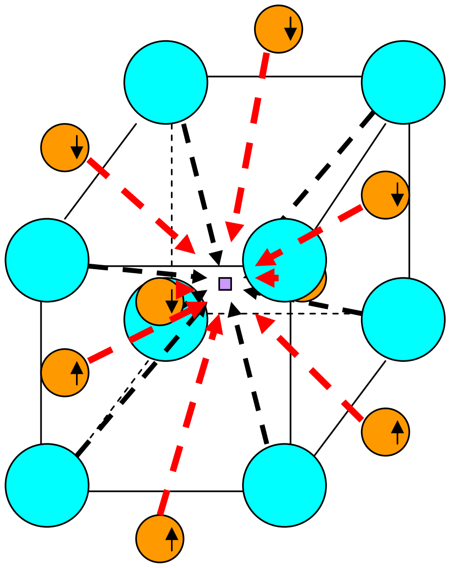

Figure 15. OSC (octahedral symmetric condensation), larger circles for deuterons, smaller circles with arrow (spin) for electrons.

$$\lambda_{2d} = {a_1}^2\lambda_{2d(1,1)} + {a_2}^2\lambda_{2d(2,2)}, \tag{4.1}$$

$$\lambda_{4d} = {a_1}^2\lambda_{4d(1,1)} + a_2^2\lambda_{4d(2,2)} + a_4^2\lambda_{4d(4,4)}, \tag{4.2}$$

$$\lambda_{8d} = {a_1}^2\lambda_{8d(1,1)} + {a_2}^2\lambda_{8d(2,2)} + {a_4}^2\lambda_{8d(4,4)} + {a_8}^2\lambda_{8d(8,8)}. \tag{4.3}$$

Here values for $\lambda_{nd(m,m)}$ intrinsic microscopic fusion rates are defined and calculated for dde*(m,m) transient molecular sates [59], and extended to multi-body fusion rates assuming rapid cascade barrier penetration and multi-body strong interactions [58–60,62]. These values are given in Table 1 of Ref. [60].

Screened Coulomb potentials for dde* EQPET molecules were calculated by the variational method of quantum mechanics [59], to be given as the following equation:

$$V_s(R) = e^2/R + V_h + (J + K)/(1 + \Delta). \tag{4.4}$$

On the right hand side of Eq. (4.4), the first term is the bare Coulomb potential and the second and third terms reflect in the screening effect by e*, which are the measure of "simply defined screening energy", as many experimentalists often use. In Table 4, effective screening energies for dde* EQPET molecules are listed up. We see that screening effects by e*(4,4) and e*(8,8) are very strong, in comparison with that a muon (mass is 208 times of electron mass) works between effects of e*(4,4) and e*(8,8). Thus, EQPET molecules may realize super screening of Coulomb potential.

In Eqs. (3.1)–(3.3), coefficients a_1–a_8 are estimated by evaluating total wave function Ψ for deuteron cluster with electrons which is expanded by wave functions $\Psi(m, m)$ of quasi-molecular states to dde*(m, m) as,

$$\Psi = a_1\Psi_{(1,1)} + a_2\Psi_{(2,2)} + a_4\Psi_{(4,4)} + a_8\Psi_{(8,8)}. \tag{4.5}$$

Table 4. Effective screening energy of dde* molecule

e*	dde*	dde*e*
(1,1)	−14.87 eV	−30.98 eV
(2,2)	−260 eV	−446 eV
(4,4)	−2460 eV	−2950 eV
(8,8)	−21 keV	−10.2 keV

In Ref. [8], approximate values of a_1–a_8 were given by taking simple quantum mechanical statistics for electron spin arrangement in TSC and OSC conditions. Calculated modal fusion rates are shown again in Table 5.

4.3. Products and Power Level of Cluster Fusion

Using modal fusion rates in Table 5, we estimated power levels of multi-body fusion rates for assumed deuteron cluster densities, as shown in Table 6. Height of periodical harmonic potential for deuteron in PdDx lattice is known to be 0.22 eV, so that 0.22 eV of deuteron (plasmon phonon) energy corresponds to excited states of trapped deuterons for dynamic motion in PdDx lattice potentials. Under this excitation condition, all deuterons trapped at O-sites move to the central T-site, and we estimate roughly the average TSC cluster density to be on the order of 10^{22} clusters per cm^3. In this condition, we get power level by 4D fusion rate to be 3 W/cm^3 (3×10^{11} f/s/cm^3) and 10 n/s/cm^3 neutron production rate by 2D fusion. Therefore neutron production rate is very small as on the 10^{-10} order of ^{4}He production rate by 4D fusion.

The OSC condition requires local PdD_2 lattice of overloaded condition, so that we assume here the OSC cluster density is very low as 10^{16} clusters/cm^3 (namely 1 ppm level of Pd atom density). Under this condition, we have still surprisingly high power level as 78 W/cm^3 (8×10^{12} f/s/cm^3) by 8D fusion rates, which produce two high-energy ^{8}Be particles per fusion.

We have speculated that 4D TSC fusion generates two 23.8 MeV ^{4}He-particles in 180° opposite directions as:

$$4\mathrm{D} \rightarrow {}^8\mathrm{Be}^*(47.6\ \mathrm{MeV}) \rightarrow {}^4\mathrm{He} + {}^4\mathrm{He} + 47.7\ \mathrm{MeV}. \tag{4.6}$$

However, we have at least once to consider the following possible branches of outgoing channels of threshold reactions for ^{8}Be (ground state) break-ups.

Table 5. Modal fusion rates for TSC and OSC

TSC (tetrahedral) (f/s/cl)	OSC (octahedral) (f/s/cl)
$\lambda_{2d} = 1.8 \times 10^{-21}$	$\lambda_{2d} = 7.9 \times 10^{-22}$
$\lambda_{3d} = 1.5 \times 10^{-13}$	$\lambda_{3d} = 3.5 \times 10^{-13}$
$\lambda_{8d} = 3.1 \times 10^{-11}$	$\lambda_{4d} = 7.0 \times 10^{-11}$
	$\lambda_{8d} = 7.8 \times 10^{-4}$

$$^{8}\mathrm{Be(g.s.)} \rightarrow {}^{4}\mathrm{He} + {}^{4}\mathrm{He} + 91.86\ \mathrm{keV}, \tag{4.7}$$

$$\rightarrow {}^{3}\mathrm{He} + {}^{5}\mathrm{He}\,(\mathrm{n} + {}^{4}\mathrm{He}) - 11.13\ \mathrm{MeV}, \tag{4.8}$$

$$\rightarrow \mathrm{t} + {}^{5}\mathrm{Li}\,(\mathrm{p} + {}^{4}\mathrm{He}) - 21.68\ \mathrm{MeV}, \tag{4.9}$$

$$\rightarrow \mathrm{d} + {}^{6}\mathrm{Li} - 22.28\ \mathrm{MeV}, \tag{4.10}$$

$$\rightarrow \mathrm{p} + {}^{7}\mathrm{Li} - 17.26\ \mathrm{MeV}, \tag{4.11}$$

$$\rightarrow \mathrm{n} + {}^{7}\mathrm{Be} - 18.90\ \mathrm{MeV}. \tag{4.12}$$

Other channels than (4.7) are threshold reactions with high threshold energies. Therefore, we have regarded these threshold reactions as minor channels with very small branching ratios, even with high-excited energy state of (4.6). Another possibility of minor channels in relation of (4.6) is break ups from excited states of ^{4}He which may break up to n + ^{3}He or t + p channels as those for 2D fusion. We regard branching ratios to these minor channels are also small, due to very steady core of alpha-clusters of ^{8}Be nucleus [63].

For 8D fusion, we can make a similar discussion that alpha-clustered channels dominate.

$$8\mathrm{D} \rightarrow {}^{16}\mathrm{O}^{*}(109.84\ \mathrm{MeV}) \rightarrow {}^{8}\mathrm{Be} + {}^{8}\mathrm{Be} + 95.2\ \mathrm{MeV}, \tag{4.13}$$

$$\rightarrow {}^{12}\mathrm{C} + {}^{4}\mathrm{He} + 50.12\ \mathrm{MeV}. \tag{4.14}$$

The life time of ^{8}Be(g.s.) is very short as 6.7×10^{-17} s to break up to two alpha-particles. Consequently, major products of 4D and 8D fusion are primarily high energy (23.8 MeV in kinetic energy) alpha-particles. The slowing down and ionization process by 23.8 MeV alpha-particles in PdDx condensed matter has very small cross section to emit K-alpha X-rays (22 keV) from Pd K-shell electron ionization. Major source of X-ray emission is speculated to the bremsstrahlung continuous X-rays in the region less than 3.5 keV by convey electrons, which are hard to observe, due to attenuation in experimental cells. Thus, energy deposit by 23.8 MeV alpha-particles becomes apparently radiation-less, namely "clean".

4.4. Secondary Reactions

High energy (23.8 MeV) alpha-particles by 4D fusion can induce secondary nuclear reactions with host metal nuclei as the following capture reactions:

Table 6. Power level of 4D and 8D fusion rates

Item	TSC (tetrahedral)	OSC (octahedral)
Density	10^{22} cl/cm^3	10^{16} cl/cm^3
Power	3 W/cm^3	78 W/cm^3
Neutron	10 n/s/cm^3	$<$ 1 n/s/cm^3

$$^{105}\mathrm{Pd} + {}^{4}\mathrm{He} \rightarrow {}^{109}\mathrm{Cd}^{*}(1.27\ \mathrm{years}), \tag{4.15}$$

$$^{106}\mathrm{Pd} + {}^{4}\mathrm{He} \rightarrow {}^{110}\mathrm{Cd}, \tag{4.16}$$

$$^{108}\mathrm{Pd} + {}^{4}\mathrm{He} \rightarrow {}^{112}\mathrm{Cd}, \tag{4.17}$$

$$^{110}\mathrm{Pd} + {}^{4}\mathrm{He} \rightarrow {}^{114}\mathrm{Cd}, \tag{4.18}$$

$$^{107}\mathrm{Pd}\,(6.5 \times 10^{6}\ \mathrm{years}) + {}^{4}\mathrm{He} \rightarrow {}^{111}\mathrm{Cd}. \tag{4.19}$$

Impurity Cd production rates in Pd cathode in the deuterium gas glow-discharge experiments by Karabut [61] may be explained by the above secondary reactions. Fission-like products also reported by Karabut [61] and Mizuno [57] can be explained by alpha-particle-induced fission process as reported by Ohta [64] in this meeting.

Even within short life of high energy ^{8}Be-particles by 8D fusion, more than ten metal nuclei exist within the range and we expect capture reactions as

$$M(A, Z) + {}^{8}\mathrm{Be} \rightarrow M(A + 8, Z + 4) + Q. \tag{4.20}$$

The kinetic energy 47.6 MeV of ^{8}Be by 8D fusion is well over the Coulomb barrier height 30.1 MeV for ^{133}Cs + ^{8}Be to ^{141}Pr reaction. Due to the liquid-drop collision-like capture process of this reaction, kinetic energy of ^{8}Be will be transferred to kinetic energy of compound nucleus $M(A + 8, Z + 4)$.

Selective nuclear transmutations reported by Iwamura [55,56] can be explained by this process, although we have few problems of possible radiation (γ-rays) emission in the process, which we will discuss elsewhere.

5. Conclusions

The EQPET model was proposed to explain super-screening for d–d pairs in condensed matter. Deuteron cluster fusion dominated will however take place by TSC and OSC conditions to make resonance multi-body fusion reactions for 3D, 4D, and 8D strong interactions. Helium-4 is the major product, and neutron production rate is very small on the order of less than 10^{-10} of helium production rate. High-energy alpha particles by 4D and 8D fusion reactions will induce secondary transmutation reactions with host or mounted heavy nuclei. Slowing down of high-energy alpha particles as products of 4D and 8D fusion reactions may emit low-energy continuous X-rays which are difficult to observe from outside of experimental cells. We can say that deuteron cluster fusion in condensed matter is clean or almost radiation-less.

References

[1] J. Huizenga, *Cold Fusion, The Scientific Fiasco of the Century* (University of Rochester Press, Rochester, 1992).
[2] *Proceedings of the First Annual Cold Fusion Conference* (University of Utah, Utah, 1990).
[3] *Proceedings of the Second Annual Cold Fusion Conference* (Italian Physical Society, Como, Italy, 1991), pp. 453–464.
[4] *Proceedings of the Third International Conference Cold Fusion* (Universal Academy Press, Nagoya, 1992), pp. 5–20.
[5] *Proceedings of the Fourth International Conference Cold Fusion*, Vol. 26, No. 4T (Fusion Technology, Maui, 1994).
[6] *Proceedings of the Fifth International Conference Cold Fusion* (Imura-E, Monte Carlo, 1995).
[7] *Proceedings of the Sixth International Conference Cold Fusion* (NEDO-Japan, Toya, 1996), pp. 425–432.
[8] *Proceedings of the Seventh International Conference Cold Fusion* (ENECO-USA, Vancouver, 1998).

[9] *Proceedings of the Eighth International Conference Cold Fusion*, Vol. 70 (Italian Physical Society, Lerici, 2001).
[10] *Proceedings of the Ninth International Conference Cold Fusion* (Springer, Beijing, 2002) (to be published).
[11] M.H. Miles, B.F. Bush, Frontier of cold fusion, *Proceedings of the ICCF2* (Universal Acadamic Press, Nagoya, 1992), pp. 189–200.
[12] Y. Arata, Y. Zhang, *J. High Temp. Soc. Jpn* **23** (1997), Special Issue.
[13] Y. Arata, Y. Zhang, *Jpn. J. Appl. Phys.* **37** (1998) L1274–L1276.
[14] M. McKubre, S. Crouch-Baker, A. Riley, S. Smedley, F. Tanzella, *Proceedings of the Third International Conference Cold Fusion* (Universal Academy Press, Nagoya, 1992), pp. 5–20.
[15] Y. Isobe, S. Uneme, K. Yabuta, Y. Katayama, H. Mori, T. Omote, S. Ueda, K. Ochiai, H. Miyamaru, A. Takahashi, Search for multi-body nuclear reactions in metal deuteride induced with ion beam and electrolysis method, *Jpn. J. Appl. Phys.* **41** (2002) 1546–1556.
[16] A. Takahashi, A. Mega, T. Takeuchi, H. Miyamaru, T. Iida, *Proceedings of the Third International Conference Cold Fusion* (Universal Academy Press, Nagoya, 1992), pp. 79–92.
[17] A. Takahashi, T. Iida, T. Takeuchi, A. Mega, *J. Appl. Electromag. Mat.* **3** (1992) 221–230.
[18] H. Fukuoka, T. Ikegawa, K. Kobayashi, A. Takahashi, *Proceedings of the Sixth International Conference Cold Fusion* (NEDO-Japan, Toya, 1996), pp. 425–432.
[19] Y. Iwamura, T. Itoh, N. Gotoh, I. Toyoda, *Fusion Technol.* **33** (1998) 476.
[20] T. Mizuno, T. Ohmori, K. Kurokawa, T. Akimoto, M. Kitaichi, K. Inoda, K. Azumi, S. Shimokawa, M. Enyo, *Denki Kagaku* **64** (1996) 1160 (in Japanese).
[21] G. Miley, J. Patterson, *J. New Energy* **1** (1996) 5.
[22] T. Ohmori, T. Mizuno, Y. Nodasaka, M. Enyo, *Fusion Technol.* **33** (1998) 476.
[23] A.B. Karabut, *Proceedings of the Eighth International Conference Cold Fusion*, Vol. 70 (Italian Physical Society, Lerici, 2001), pp. 329–340.
[24] Y. Iwamura, T. Itoh, M. Sakno, S. Sakai, Observation of low energy nuclear reaction induced by D2 gas permeation through multi-layer Pd film, *Proceedings of the Ninth International Conference Cold Fusion* (Springer, Beijing, 2002) (to be published).
[25] T. Itoh, M. Sakano, S. Sakai, Y. Iwamura, ibid.
[26] M. Sakano, T. Itoh, S. Sakai, Y. Iwamura, ibid.
[27] Y. Iwamura, T. Itoh, M. sakano, S. Sakai, *Jpn. J. Appl. Phys.* **41** (2002) 4642–4650.
[28] V.A. Chechin, V.A. Tsarev, M. Rabinowitz, Y.E. Kim, *Int. J. Theor. Phys.* **33** (1994) 617–670.
[29] S. Chubb, T. Chubb, *Fusion Technol.* **17** (1990) 710.
[30] A. Takahashi, T. Iida, F. Maekawa, H. Sugimoto, S. Yoshida, *Fusion Technol.* **19** (1991) 380.
[31] A. Takahashi, T. Iida, H. Miyamaru, M. Fukuhara, *Fusion Technol.* **27** (1995) 71.
[32] A. Takahashi, Drastic enhancement of tetrahedral and octahedral resonance fusion under transient condensation of deuterons at lattice focal points, *Proceedings of the Ninth International Conference Cold Fusion* (Springer, Beijing, 2002) (to be published).
[33] V. Kirkinskii, Y. Novikov, *Theoretical Modeling of Cold Fusion* (Novosibirsk University Publications, Novosibirsk, 2002).
[34] V. Violante, C. Sibilia, D. Di Giacchino, M. Mckubre, F. Tanzara, P. Tripodi, *Proceedings of the Eighth International Conference Cold Fusion*, Vol. 70 (Italian Physical Society, Lerici, 2001), pp. 409–418.
[35] A. Takahashi, *J. Nucl. Sci. Technol.* **26** (1989) 558.
[36] M. Fleischmann, S. Pons, *J. Electroanal. Chem.* **261** (1989) 301.
[37] A. Takahashi, K. Maruta, K. Ochiai, H. Miyamaru, T. Iida, *Fusion Technol.* **34** (1998) 256.
[38] A. Takahashi, K. Maruta, K. Ochiai, H. Miyamaru, *Phys. Lett. A* **255** (1999) 89–97.
[39] Y. Isobe, S. Uneme, K. Yabuta, H. Mori, T. Omote, S. Ueda, K. Ochiai, H. Miyamaru, A. Takahashi, *Proceedings of the Eighth International Conference Cold Fusion*, Vol. 70 (Italian Physical Society, Lerici, 2001), pp. 17–22.
[40] T. Dairaku, Y. Katayama, T. Hayashi, Y. Isobe, A. Takahashi, *Proceedings of the Ninth International Conference Cold Fusion* (Springer, Beijing, 2002) (to be published).
[41] G. Preparata, *Proceedings of the Second Annual Cold Fusion Conference* (Italian Physical Society, Como, 1990), pp. 453–464.
[42] F. Celani, A. Spallone, P. Tripodi, D. Di Gioacchino, P. Manini, A. Mancini, *Proceedings of the Sixth International Conference Cold Fusion* (NEDO-Japan, Toya, 1996), pp. 228–233.